



Water Research Center (WRC), University of Khartoum (UofK)

AU-NEPAD CEANWATCE ACEWATER2 PROJECT

WATER and COOPERATION within the Nile River Basin (WACONI)

Blue Nile Basin Downstream the Grand Ethiopian Renaissance Dam

**Water-Energy-Food-Ecosystem nexus
assessment**

Coordinator: Prof. Gamal Abdo

September 2019

Table of contents

Table of contents.....	I
List of tables	II
List of figures.....	III
List of Abbreviations.....	IV
1. Summary	1
2. Introduction	2
2.1. Background.....	2
2.2. Literature review.....	3
2.3. Scope	6
3. Study area	7
3.1. Extent	7
3.2. Dams.....	7
3.2.1. Sennar Dam.....	7
3.2.2. Roseires Dam.....	8
3.2.3. The operation of the Sennar and Roseires dams.....	9
3.2.4. The Grand Ethiopian Renaissance Dam	10
3.3. Irrigation schemes.....	11
3.4. Water use rights.....	12
4. Data used	14
4.1. Spatially distributed data	14
4.1.1. Average monthly evapotranspiration	15
4.1.2. Topography.....	16
4.2. Descriptive data	17
4.2.1. Reservoir geometry	17
4.2.2. Reservoir evaporation coefficients.....	19
4.2.3. Dam outlet specifications.....	20

4.3. Geographic data.....	20
4.3.1. Existing and planned irrigation schemes.....	21
4.3.2. Hydraulic structures.....	21
4.3.3. River streams.....	21
4.3.4. Natural reserves.....	21
4.3.5. Weather and flow stations.....	22
4.4. Point data.....	23
4.4.1. Monthly rainfall.....	23
4.4.2. Average daily river flow.....	24
4.4.3. Average monthly water abstractions.....	25
5. Water-energy-food-ecosystem nexus modeling.....	26
5.1. Model components.....	26
5.2. Modeling framework.....	27
5.3. Evaluation of satellite-based rainfall products.....	29
5.4. Model performance.....	33
5.5. Simulation scenarios.....	38
6. Water-energy-food-ecosystem nexus assessment.....	40
6.1. River flow.....	40
6.2. Energy generation and water-energy productivity.....	41
6.3. Irrigation water supply.....	43
6.4. Water supply to the ecosystem.....	44
7. Conclusions and way forward.....	46
8. References.....	47

List of tables

Table 1 Picture and main features of the Sennar dam.....	8
--	---

Table 2 Picture and main features of the Roseires dam	9
Table 3 Summary of the main features of the Grand Ethiopian Renaissance Dam	10
Table 4 Nile Water Agreements in chronological order	12
Table 5 Major water abstraction in the study area	25
Table 6 Methods used for simulating various processes	29
Table 7 Model performance at three locations in the study area	38

List of figures

Figure 1 Nile Basin boundary and sharing countries	3
Figure 2 General features of the Blue Nile Basin downstream the GERD	7
Figure 3 Irrigation schemes in the study area	12
Figure 4 Architecture of the database	14
Figure 5 Average monthly evapotranspiration in the study area	16
Figure 6 Topography of the study area	17
Figure 7 Geometry of the reservoirs in study area	18
Figure 8 Net evaporation of the reservoirs in study area	19
Figure 9 Total release capacity of the three dams in the study area	20
Figure 10 Location of the Dinder National Park	22
Figure 11 River and weather stations in the study area	23
Figure 12 Average monthly rainfall at five stations in the study area	24
Figure 13 Average daily river flow at four stations in the study area	24
Figure 14 Schematic of the water balance model	27
Figure 15 Modeling framework used in this study	28
Figure 16 Rainfall stations used in this study	30
Figure 17 Performance metrics of the evaluated satellite-based rainfall products	32
Figure 18 Overall performance of the satellite-based rainfall products in the study area	33

Figure 19 Daily observed and simulated outflow from the Roseires Dam: (a) time series for the calibration and validation periods (b) scatter plot of the calibration period, and (c) scatterplot of the validation period.....35

Figure 20 Daily observed and simulated outflow from the Sennar Dam: (a) time series for the calibration and validation periods (b) scatter plot of the calibration period, and (c) scatterplot of the validation period.....36

Figure 21 Daily observed and simulated flow at the Khartoum Gage: (a) time series for the calibration and validation periods (b) scatter plot of the calibration period, and (c) scatterplot of the validation period.....37

Figure 22 Scenarios modeled in this study38

Figure 23 Historic standardized streamflow index of the Blue Nile at the Eldiem gage.40

Figure 24 Exceedance probability of the Blue Nile flow at Eldiem with and without the GERD.41

Figure 25 Parallel plots of the historic annual (1984-2016) water-energy-food-ecosystem nexus indicators.....42

Figure 26 Steady-state energy generation from the Grand Ethiopian Renaissance Dam...43

Figure 27 Parallel plots of the historic (1984-2016) water-energy-food-ecosystem nexus indicators.....44

Figure 28 Parallel plots of the historic (1984-2016) water-energy-food-ecosystem nexus indicators.....45

List of Abbreviations

ARC 2.0	African Rainfall Climatology Version 2
CEANWATCE	Central/Eastern Africa Network of Water Centers of Excellence
CHIRPS 2.0	Climate Hazards group Infrared Precipitation with Stations version 2.0
DIU	Dams Implementation Unit
FAO	Food and Agriculture Organization
FSL	Full Supply Level
GERD	Grand Ethiopian Renaissance Dam

HEC	Hydrologic Engineering Center
HMS	Hydrologic Modeling System
IWMI	International Water Management Institute
MIT	Massachusetts Institute of Technology
MOD16	Moderate Resolution Imaging Spectroradiometer Global Evapotranspiration Project
MoiHES	Ministry of Irrigation and Hydro-Electric Energy of Sudan
MoiHPS	Ministry of Irrigation and Hydro-Electric Power of Sudan
NSE	Nash–Sutcliffe Efficiency
MPE	Mean Percentage Error
NBI	Nile Basin Initiative
PERSIANN-CDR	Precipitation Estimation from Remotely Sensed Information Using Artificial Neural Networks–Climate Data Record
R²	coefficient of determination
SRTM	Shuttle Radar Topography Mission
TAMSAT 2	Tropical Applications of Meteorology Using Satellite Data and Ground-Based Observations version 2
WEFE	Water, Energy, Food, and Ecosystems
WRC	Water Research Center

1. Summary

This study analyzes the water-energy-food-ecosystem (WEFE) nexus in the Blue Nile Basin in Sudan and assesses the impact of the Grand Ethiopian Renaissance Dam (GERD). Water availability, hydropower generation, irrigation water supply, and environmental flows are the components considered in the assessment. A calibrated daily rainfall-runoff (HEC-HMS) and water allocation (RIVERWARE) model was used to quantify the four nexus components and their interlinkages. The model was calibrated for the period 1984 – 2000 and validated for the period 2001 - 2016, and includes three storage reservoirs (GERD, Rosaries Dam and Sennar Dam), seven inflow nodes, five irrigation demand nodes, evaporation losses from reservoirs, return flows from irrigation, and transmission losses from river reaches. 34 simulation scenarios were examined which comprise a historic baseline scenario for the 1984 – 2016 period and a scenario with GERD on the river system. The latter scenario was examined across 33 hydrologic conditions developed using the index-sequential method (Kendall and Dracup, 1991; Ouarda et al., 1997). Due to a scarcity of ground rainfall data in the study area, a pixel-to-point evaluation was conducted for four satellite-based rainfall products and the best-performing one was used as a boundary condition for the rainfall-runoff component of the model. The evaluated satellite rainfall products include the African Rainfall Climatology Version 2 (ARC2.0), the Tropical Applications of Meteorology Using Satellite Data and Ground-Based Observations version 2 (TAMSAT2), the Precipitation Estimation from Remotely Sensed Information Using Artificial Neural Networks–Climate Data Record (PERSIANN-CDR), and the Climate Hazards group Infrared Precipitation with Stations version 2.0 (CHIRPS 2.0). The suit of models developed herein was used to assess the historic and future association of seven WEFE nexus indicators.

The results show a historic association between environmental flow supply, irrigation water supply, and water availability. The heightening of the Roseires Dam in 2013 affected most of the nexus indicators. The analysis shows that the steady-state operation of the Grand Ethiopian Renaissance Dam will positively impact irrigation water supply, hydropower generation, and environmental flows in the Blue Nile Basin in Sudan.

2. Introduction

2.1. Background

It is now widely acknowledged that bridging the gap between human ingenuity and the challenge of resources scarcity using an integrated approach as opposed to fragmented approaches is crucial to assure the long term water-energy-food-ecosystem (WEFE) Sustainability (Hoff, 2011). The resources scarcity challenge can be described by two conditions the world is going through in the present-day: on one side, the rapidly swelling urbanization that is escorted by an incredible growth of the middle-income group and the significant changes in lifestyles. Specifically, in the year 1950 around one-third of the world's population lived in cities, while in the year 2000 nearly half were city dwellers and they will increase furthermore to two-thirds by the year 2030 which indicates a high growth rate of the middle-income group (UNDP, 2015). At the same time, It is projected that the global population will grow to 8.5 billion by the year 2030, 9.7 billion by the year 2050, and 11.2 billion by the year 2100 (UN, 2015a). Moreover, about 800 million people are living in extreme poverty and suffer from hunger, approximately 1.2 billion people have income lower than 1.25 USD per day (Bhattacharyya et al., 2015) and above 160 million children under age five have inadequate height for their age attributable to insufficient food (UN, 2015b). On top of that, water scarcity is affecting more than 40 percent of the people around the world. These effects will be progressively amplified by climate change, which could expose around 250 million people to greater water stress in Africa alone (UNDP, 2015). In 2015, it was estimated that 844 million people worldwide still use unimproved drinking water sources, including unprotected wells, springs, and surface water (UN, 2018).

The Nile is the longest river in the world with 6700 km length. Its watershed covers approximately 10 % of the African continent and 2 % of the Earth's land surface with around 3.3 million km² extending over 11 countries in Africa. These countries are Burundi, Rwanda, Democratic Republic of Congo, Tanzania, Uganda, Kenya, Sudan, South Sudan, Ethiopia, Eritrea, and Egypt (Mohamed and Louseged, 2008; Ribbe and Ahmed, 2006). Figure 1 illustrates the Nile Basin boundary and the sharing countries.

The farthest source of the Nile is the Ruvyironza River which originates in Burundi and flows into Lake Victoria from which the Victoria Nile arises and travels northwards passing through Lake Kyoga and then into Lake Albert. After that, the River re-emerges from Lake Albert as the Albert Nile, continues the Journey northwards, and passes the South Sudanese Ugandan border. From that point, it is known as Bahr Eljebel. In the South Sudanese territories, Bahr Eljebel flows into the Sudd swamps. The River re-emerges from the Sudd swamps and meets the Sobat River which originates in Ethiopia in the east. The resulting river is known as the White Nile, which flows northward until it finally meets the Blue Nile at Khartoum, the capital of Sudan (NBI, 2012). The Blue Nile, which originates from Lake

Tana in Ethiopia, is fed by many tributaries between its origin and its confluence point with the White Nile. Its major tributaries are the Rahad and Dinder, which also originate in the Ethiopian Highlands (NBI, 2012). From Khartoum, the Main Nile flows northwards and joins by the Atbara River which also originates in the Ethiopian Highlands. The combined rivers continue flowing crossing the Sahara desert through Egypt and in the end, discharges into the Mediterranean Sea (NBI, 2012). In this study, the WEF nexus framework will be used to understand the past and future linkages of the nexus resources in the Blue Nile Basin in Sudan.

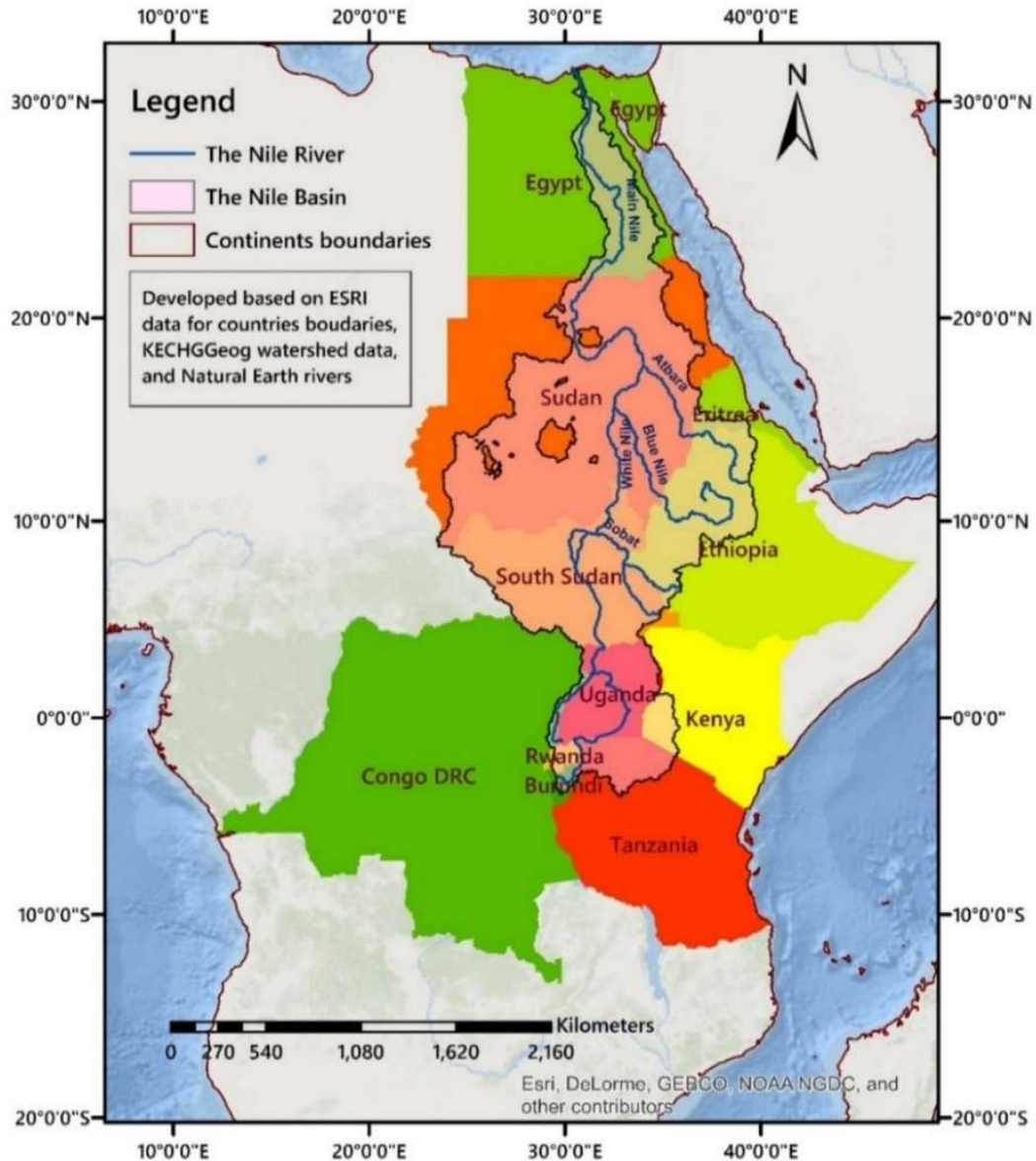


Figure 1 Nile Basin boundary and sharing countries

2.2. Literature review

The emerging WEF nexus theoretical framework illustrates a clear need to advance our understanding of the interactions between water use and management, energy production, food production, and environmental requirements. This knowledge is pivotal to circumvent future supply deficiencies that would hinder development and to ensure access to water, energy, and food while maintaining the environment in an acceptable status. Dams ostensibly show that the interdependencies of water, energy, and food depend on a reliable, incessant, and effectual supply of water. Therefore, the operation rules of dams play a principal role in the WEF nexus (Lindström and Granit, 2012).

In recent years, a considerable amount of literature investigated the applicability of the WEF nexus approach on transboundary river basins. Bazilian et al. (2011) studied the interlinkages of WEF from a developing country perspective and argued that holistic treatment of the three resources in transboundary river basins results in improved allocation, economic efficiency, and minimization of negative externalities. Nevertheless, it was found that tools and expertise are not “yet” available to bring the WEF nexus approach into practice (Bazilian et al., 2011). The results of another study, which applied the WEF nexus approach on the Mekong River Basin, revealed that water and food security are likely to be altered by current hydropower development plans in the Mekong River Basin (Keskinen et al., 2015). Moreover, Keskinen et al. (2015) and Strasser et al. (2016) compared the Integrated Water Resources Management and the WEF nexus approaches and concluded that the WEF nexus approach treats WEF sectors in an equal manner. However, it was found that some other aspects such as livelihoods, climate change, and the environment are not included in the WEF nexus approach (Keskinen et al., 2015). To fill these gaps, further methodologies were developed accounting for missing facets. Kibaroglu and Gürsoy (2015) studied the evolution of transboundary WEF management policies in the Euphrates–Tigris River Basin and their impacts on cooperation between riparian countries. These authors found that the compound nature of pressures and drivers in the Euphrates–Tigris River Basin necessitates adopting a nexus approach to provide mutual benefits for riparian countries. Pittock et al. (2016) developed a comprehensive WEF nexus influence framework for the Mekong River Basin that shows the impacts of changing any variable in the river system on the WEF nexus. Strasser et al. (2016) proposed a methodology to assess water-energy-food-ecosystem nexus in transboundary river basins and presented results from its application on the Alazani/Ganykh, the Sava, and the Syr Darya transboundary river basins.

Assessing the WEF nexus is often carried out by separate disconnected institutional entities. For instance, water management institutions are likely to treat food and energy production as end users, food and agricultural institutions see water and energy as production inputs, whereas energy institutions treat water as a resource (Howells et al., 2013). The need for the WEF nexus approach originated from the growing scarcity which

resulted in strengthening the interlinkages of the three resources, recent supply crises of the three resources, and failures of individualism in sectorial management (Al-Saidi and Elagib, 2017). While the integrated management view of the water, food, energy, and the environment is a new approach which has recently started in the 2000s, the demand for water-food, water-energy, and food-energy nexuses date back to programs in the 1980s by the United Nations University (Bhattacharyya et al., 2015). The Water, Energy, Health, Agriculture, and Biodiversity (WEHAB) working group developed a framework for the nexus of Water, Energy, Health, Agriculture, and Biodiversity during the Johannesburg 2002 earth summit. The WEHAB framework put energy in the center and showed its interlinkages with other sectors without showing how the other sectors are connected (WEHAB Working Group, 2002). Similar to the Johannesburg framework, more recently, the Bonn Nexus Conference in 2011 has approached the problem from a water security perspective putting the available water resources in the center of the nexus (Hoff, 2011). The World Economic Forum (2011) emphasized on the risk associated with the three resources. Environmental pressures, Governance failures in terms of managing shared resources such as transboundary water sources, and Economic disparity, which often results in intensive use of resources, are considered as drivers to the risks. As part of the FAO vision of eradicating hunger, reducing poverty, and managing resources sustainably, the FAO created a WEF nexus framework (Flammini et al., 2014). Lindström & Granit (2012) provided an overview of the-state-of-the-art of large-scale artificial water storage and its role in the WEF nexus. The study showed the challenges and potential benefits of different storage options. Moreover, it analyzed the potential negative impacts of different storage options on populations and the local environment. Another framework named Climate, Land-Use, Energy, and Water Strategies (CLEWS) utilized existing well-tested assessment tools and methodologies in modeling the interlinkages of WEF (Howells et al., 2013). A module-based tool was developed in which data are passed between different tools in an iterative fashion (Howells et al., 2013).

The nexus approach did not have much attention in Africa compared to other regions in the world. Endo et al. (2017) review a number of water, energy, food, and climate related studies on Africa to see their nexus orientation. They found that most of the studies on Africa did not include all the nexus side. Some nexus research has been recently conducted for the Nile Basin. Basheer and Elagib (2018a) examined the water-energy nexus for the White Nile and the Jebel Aulia Dam. They introduced the water-energy productivity, which is defined as the amount of water lost to evaporation from a reservoir for each unit of hydro-energy generation. They used this water-energy nexus indicator to explore better ways to operate the Jebel Aulia Dam. Basheer et al. (2018) explored the impacts of transboundary cooperation in the Blue Nile Basin on the water-energy-food nexus. The authors found that a higher level of cooperation results in more benefits for the basin. Elagib et al. (2019) investigated the urban water-energy-food nexus in Khartoum State at

the colfulence of the Blue Nile and the While Nile. They found a strong relation between hydrological phenomenon (such as flood and drought) and resources nexus. Stamou and Rutschmann (2018) analyzed the trade-offs and synergies between hydropower generation and irrigation water supply in the Upper Blue Nile Basin using the parameterization-simulation-optimization method.

2.3. Scope

Given the limited water resources of the Nile Basin and the many challenges related to WEFE, the Central/Eastern Africa Network of AU/NEPAD Water Centers of Excellence (CEANWATCE) selected the Nile Basin as a study region in the framework of ACEWATER2 project. Two case studies were selected: the Blue Nile Basin and the Lake Victoria Basin. The Water Research Center (WRC) of the University of Khartoum studied the hydrology and water allocation of the Blue Nile Basin downstream the GERD (see Figure 2) intending to assess the impacts of infrastructural developments on the inter-linkages of the WEFE.

3. Study area

3.1. Extent

The study area extends over the Blue Nile reach from the GERD location until the confluence point of the Blue Nile and the White Nile (see Figure 2). It includes all water inflows and abstractions to and from the Blue Nile reach covered by the study area. Although there is a considerable additional runoff between the GERD and Roseires dam, usually little additional runoff north of Roseires add to the Blue Nile due to a relatively lower rainfall in this region. The exceptions are the Dinder and the Rahad Rivers, which join the Blue Nile downstream of Sennar dam (Abd Elrahim, 2012; ENTRO, 2006).

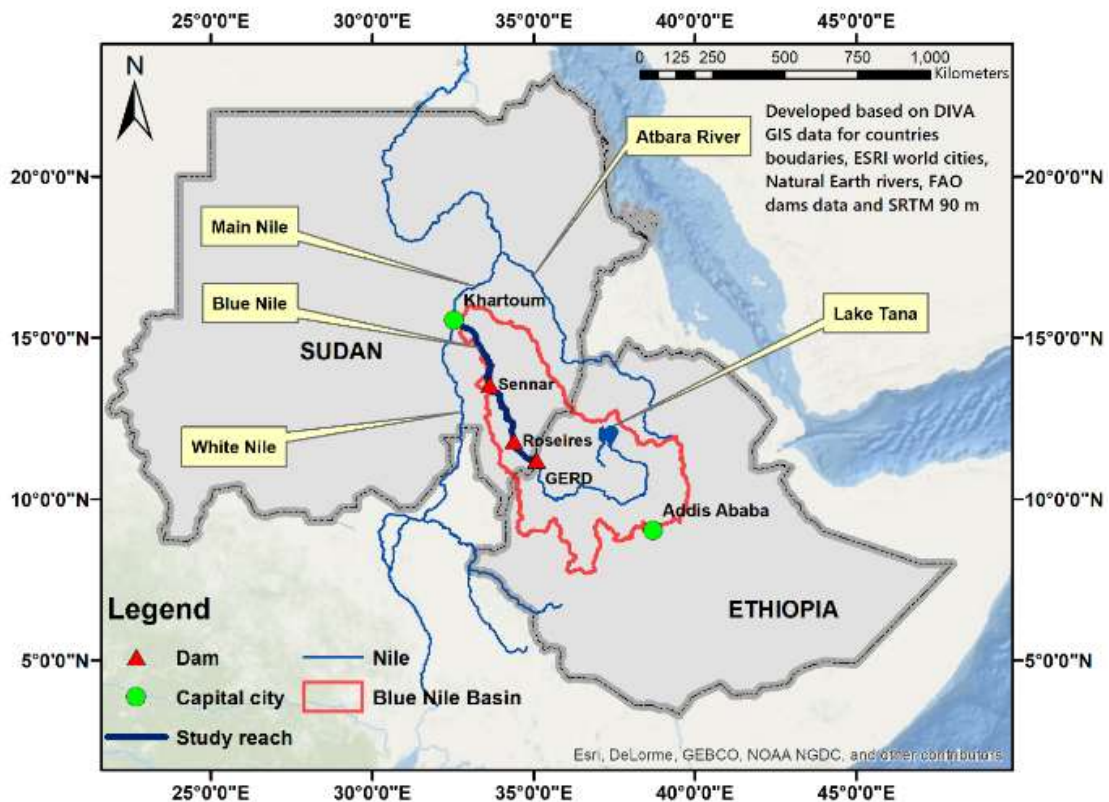


Figure 2 General features of the Blue Nile Basin downstream the GERD


3.2. Dams

3.2.1. Sennar Dam

The Sennar Dam, located on Blue Nile River some 350 km southeast Khartoum, became operational in 1925 to supply 126,000 ha of cotton in the Gezira scheme with irrigation

water by gravity from head works located within the dam on the left bank of the Blue Nile. In 1959, a study was carried out to investigate the possibility of raising the Sennar Reservoir by 4 meters. This study showed that without major works, large portions of many villages, towns and pumped irrigation schemes would be flooded, and the proposal was taken no further. In 1962 two 7.5 MW turbines were installed in a power station on the west side of the dam to utilize the downstream flow for hydropower generation (MoIHES, 1977). The general characteristics of Sennar dam are summarized in Table 1 below.

Table 1 Picture and main features of the Sennar dam


	Reservoir Data Full Supply Level (FSL)	421.7 masl
	Minimum operating level (MOL)	417.2 masl
	Lowest Drawdown Level	416
	Operating range	4.5 m
	Total storage volume	640 MCM (in 1985)
	Live storage volume	420 MCM
	Dead storage volume	220 MCM
	Surface area at FSL	160 BCM
	Surface area at MOL	95 km ²
	Hydropower Power station	2 turbines of 15 MW
Average annual energy	100 GWh	
Release capacity At FSL	950 MCM/day	
At MOL	1470 MCM/day	

3.2.2. Roseires Dam

The implementation of the Managil extension of the Gezira Scheme led the Sudanese government in the year 1925 to investigate a proposal for the construction of a dam with a capacity of at least 1.0 BCM near the Roseires Town. Two years later the location of the dam was confirmed, and the MOL was decided to be 471.5 masl. The provision of storage larger than 1.0 BCM stood out to be important, especially after the completion of the Managil extension. Therefore, in 1955 the Sudanese government appointed the firms of Sir Alexander Gibb & Partners and Coyne et Bellier of Paris to conduct a joint study on the consequences of constructing a larger dam at Roseires than the one proposed earlier in 1925. The two firms suggested a design for a dam that would be constructed in two stages, the first stage with a MOL of 480 masl and the second stage with a MOL 10.0 meters higher than the first stage (MoIHPS, 1966).

The first stage of the dam was completed in the year 1966 followed by an attempt to construct the second stage in the 1990s which stopped because of the economic situation of Sudan at that time (Roseires Dam Heightening Unit, 2005). The heightening of the dam started again in May 2009 and was finished in January 2013 (DIU, 2016). Table 2 below shows the general features of the Roseires dam after the completion of the second stage.

Table 2 Picture and main features of the Roseires dam

	Dam design data Total average annual flow of the Blue Nile at Roseires	50 BCM
	Reservoir Data FSL MOL Operating range Total storage volume Live storage volume Surface area at FSL Surface area at MOL	490 masl 467 masl 23 m 5.9 BCM (in 2012) 5.87 BCM 564 km ² 10.5 km ²
	Irrigation Potential Kenana canal Dinder canal	Maximum discharge 360 m ³ /s
	Powerhouse Units number Installed power capacity Average annual energy after heightening	7 280 MW 2200 GWh
	Release capacity At FSL At MOL	701 MCM/day 2585 MCM/day

3.2.3. The operation of the Sennar and Roseires dams

The water stored in Roseires and Sennar dam is essential in irrigating the Blue Nile agricultural schemes since the flows of the Blue Nile, and its tributaries are limited during the dry season. In addition to providing agricultural water, Roseires and Sennar dams serve in hydropower production. Considering the limits on water abstraction permitted by the Egypt-Sudan agreement of 1959, the Sudanese authorities aim to maximize the benefit from irrigation and hydropower while minimizing the sedimentation to reduce the

maintenance cost and to prolong the lifetime of the two reservoirs (Sutcliffe and Parks, 1999).

The operation rules of both the Roseires and Sennar dams are related to the natural flow of the Blue Nile measured at Eldeim near the Sudanese Ethiopian border. Allowance is made for transmission losses, which include evaporation and percolation losses. This allowance is 1% of El Deim flow for the reach from El Deim to the beginning of Roseires reservoir and 2% of the Roseires outflow for the reach from Roseires to Sennar reservoirs. Additionally, the Sennar outflow should not be less than 8 MCM per day in order to meet the environmental flow requirements.

3.2.4. The Grand Ethiopian Renaissance Dam

The idea of the Grand Ethiopian Renaissance Dam (GERD) dates back to 1964 after the study conducted by the US Bureau of Reclamation on the utilization of the Blue Nile by Ethiopia which recommended the construction of a dam with 11 BCM storage capacity at the current location of the GERD. The project was not implemented at that time due to political, diplomatic, technical, and economic limitations of Ethiopia. Since 1999, by participating in the NBI, Ethiopia tried to get the necessary funds for constructing the dam. In 2008, pre-feasibility studies for the GERD (was called the Border dam at that time and had a storage capacity of 14.5 BCM) was supposed to be prepared but disagreement over the cooperation framework and the consequent suspension of Egypt’s membership from the NBI have delayed the implementation of the project (Mohammed, 2015; Tawfik, 2016).

On April 2, 2011, the Ethiopian government announced the start of the currently under construction GERD with a power capacity ranked as the largest in Africa and the tenth largest globally. The GERD is located on the Blue Nile River 20 kilometers upstream of the Sudanese Ethiopian border and is being constructed by Salini Impregilo -an Italian construction company- with a total cost of around 4.8 billion USD (Salini Impregilo, 2016; Salman, 2016; Swanson, 2014). The dam is a roller compacted concrete with a height of 145 meters complemented by a saddle dam about 5 km long and about 50 m high (MIT, 2014). Table 3 below summarizes the main characteristics of the GERD.

Table 3 Summary of the main features of the Grand Ethiopian Renaissance Dam

Hydrological data	
Catchment area	172,250 km ²
Mean annual flow	1547 m ³ /s
Reservoir Data	
FSL	640 masl
MOL	590 masl
Operating range	50 m

Total storage volume	74.01 BCM
Live storage volume	59.22 BCM
Surface area at FSL	1,874 km ²
Surface area at MOL	606 km ²
Mean annual sediment yield	207 MCM/year
Length of the reservoir at FSL	246 km
Powerhouse	
Units number/Type	16/ Francis
Installed power capacity	6,450 MW
Average annual energy generation	15,692 GWh/ year
Plant factor	0.31
Spillway	
Design capacity	15,000 m ³ /s
Sluices	6 sluices (14 x 15.5 m)

3.3. Irrigation schemes

Figure 3 depicts the irrigation schemes in the study area. Large-scale agricultural development began in 1925 with the construction of Sennar Dam and the commissioning of the Gezira Scheme. During the late 1950s and 1960s, the Managil extension was constructed which more than doubled the total area of the Gezira. The total area of Gezira and Managil schemes amounts to around 840,000 Ha. The Gezira and Managil remain the only gravity-fed scheme based on the Blue Nile and represent more than 50 percent of irrigated agriculture in Sudan. The Gezira and Managil are considered as the largest irrigation schemes in the world managed under one administrative unit (MoIHES, 1977).

Weighty development in pumping irrigation abstracting from the Blue Nile took place in the 19th century. However, it was only carried out by a private initiative in reaction to the 1950s increase in cotton prices. The end of the cotton prices explosion and other complications steered the deterioration in many of the Blue Nile pumping schemes and, partly because of this, some of them were nationalized in the late 1960s. The Blue Nile pumping developments include the construction of the Gunied, Rahad phase1, and Suki Schemes which took place during the late 1960s in addition to North West Sennar Sugar scheme in the 1970s (IWMI, 2012; MoIHES, 1977).

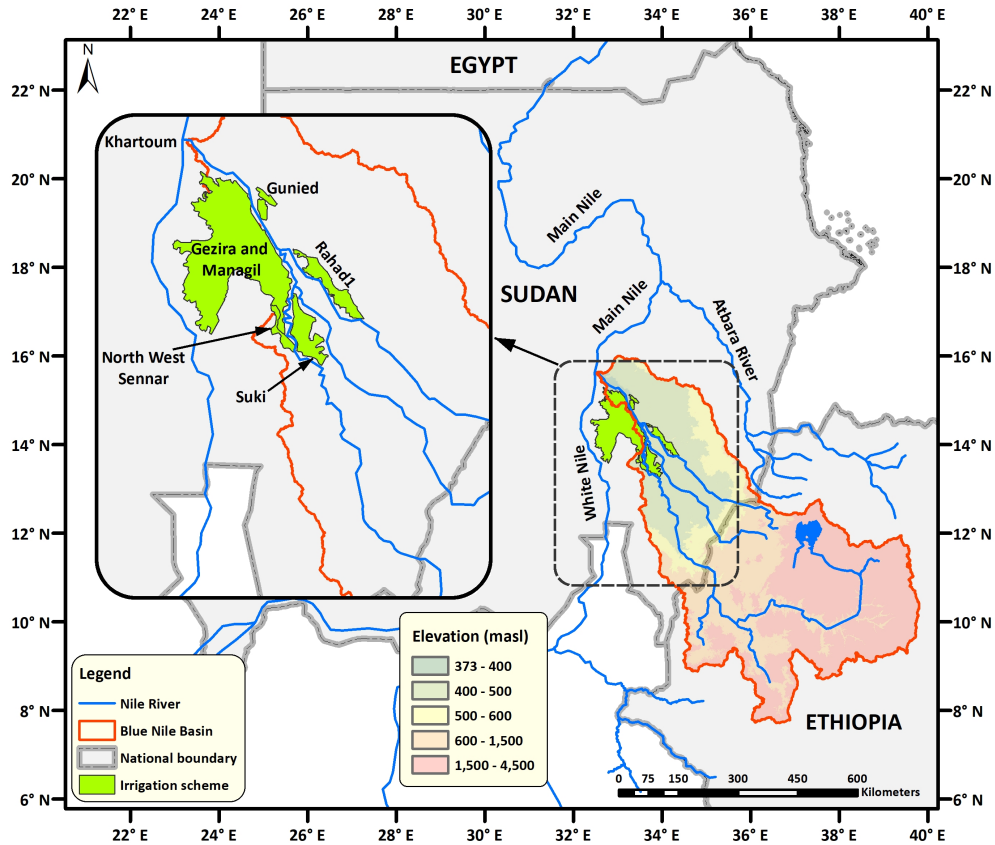


Figure 3 Irrigation schemes in the study area

3.4. Water use rights

Table 4 below gives a brief account of the Nile Water Agreements governing the uses and the sharing of Nile waters in chronological order. It worth mentioning that the colonizing forces signed most of the agreements below on behalf of their colonies.

Table 4 Nile Water Agreements in chronological order

Agreement	Year
Protocol between Britain and Italy	1891
Treaty between Britain and Ethiopia	1902
Agreement between Britain and Congo	1906
Agreement between Britain, Italy and Ethiopia	1906
Exchange of notes between Britain and Italy	1925
Nile water agreement	1929
Convention between Britain and Belgium	1934

Agreement	Year
Exchange of memoranda between Egypt and Great Britain	1949-1953
Egypt and the Sudan Nile Agreement	1959
Exchange of memoranda between Egypt and Uganda	1991
Framework for General Cooperation between Egypt and Ethiopia	1993
Agreement between Egypt and Uganda for controlling water hyacinth	1998
Agreement on Declaration of Principles between Sudan, Egypt, and Ethiopia	2015

Note: Adapted from (DoP, 2015; UNEP, 2010)

The 1959 treaty between Sudan and Egypt resulted in the construction of the High Aswan dam and increased the water allocated to the two countries. It stated, “The total share from the net yield of the Nile shall be 18.5 BCM for Sudan and 55.5 BCM for Egypt”. The recently signed declaration of principles between Ethiopia, Sudan, and Egypt on the GERD consist of 10 principles that show a willingness to cooperate (DoP, 2015). Four of the principles are related to the GERD, while the rest are principles of international water law (Salman, 2016). The ten principles are:

- Principle of cooperation
- Principle of development, regional Integration, and Sustainability
- Principle equitable and reasonable utilization
- Principle of not to cause significant Harm
- Principle to cooperate on the first filling and operation of the GERD
- Principle of confidence building
- Principle of exchange of information and data
- Principle of dam safety
- Principle of sovereignty and territorial integrity
- Principle of peaceful settlement of disputes

4. Data used

This study uses several kinds of data that have been collected through the project period. The key data that have been used in this study are organized in an online database. The architecture of the database is designed as indicated in Figure 4 below. Due to the large size of some of the data and to ease data sharing and distribution between the project partners, the data have been categorised and uploaded to a Dropbox Folder. Then a Portable Document Format (PDF) file has been created to act as an entry point to the database. The PDF file is provided with this report but separately. The PDF file includes the flow chart illustrated in Figure 4. Through the PDF file, the user can view or download the data. The database contains several data formats such as Excel files, shapefiles, and raster files. Clicking on any of the boxes in the PDF file opens the respective data folder on Dropbox. The database includes four main data categories: (1) spatially distributed data, (2) descriptive data, (3) geographic data, and (4) point data. Each of the four categories includes sub-categories. The following part of the report describes the data within each category and their sources.

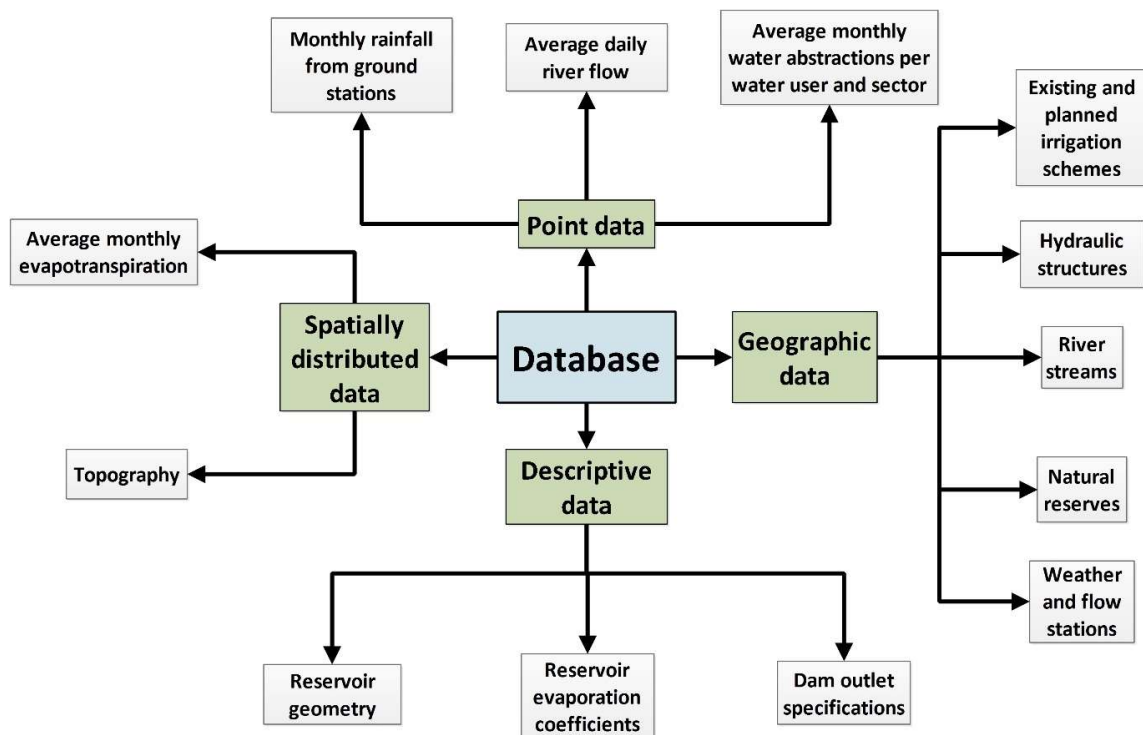


Figure 4 Architecture of the database

4.1. Spatially distributed data

The database includes two types of spatially distributed data which are average monthly evapotranspiration and topography.

4.1.1. Average monthly evapotranspiration

Figure 5 shows the average monthly evapotranspiration in the Blue Nile Basin. Average monthly evapotranspiration was calculated for the Blue Nile Basin based on the Moderate Resolution Imaging Spectroradiometer Global Evapotranspiration Project (MOD16; Mu et al. (2011)). MOD16 is a satellite-based evapotranspiration product that covers the globe with monthly data for the period 2000 to 2014. The product has a 1 km × 1 km spatial resolution. The University of Montana developed MOD16 as part of NASA/EOS Project. The evapotranspiration data provided by MOD16 includes direct evaporation from wet and moist soil plus transpiration from vegetation during daytime and nighttime. Herein, the data are added to the database in a Raster (GeoTiff) format and has a unit of 0.1mm/month. Moreover, the data are provided in the World Geodetic System 1984 (WGS84) geographic coordinate system.

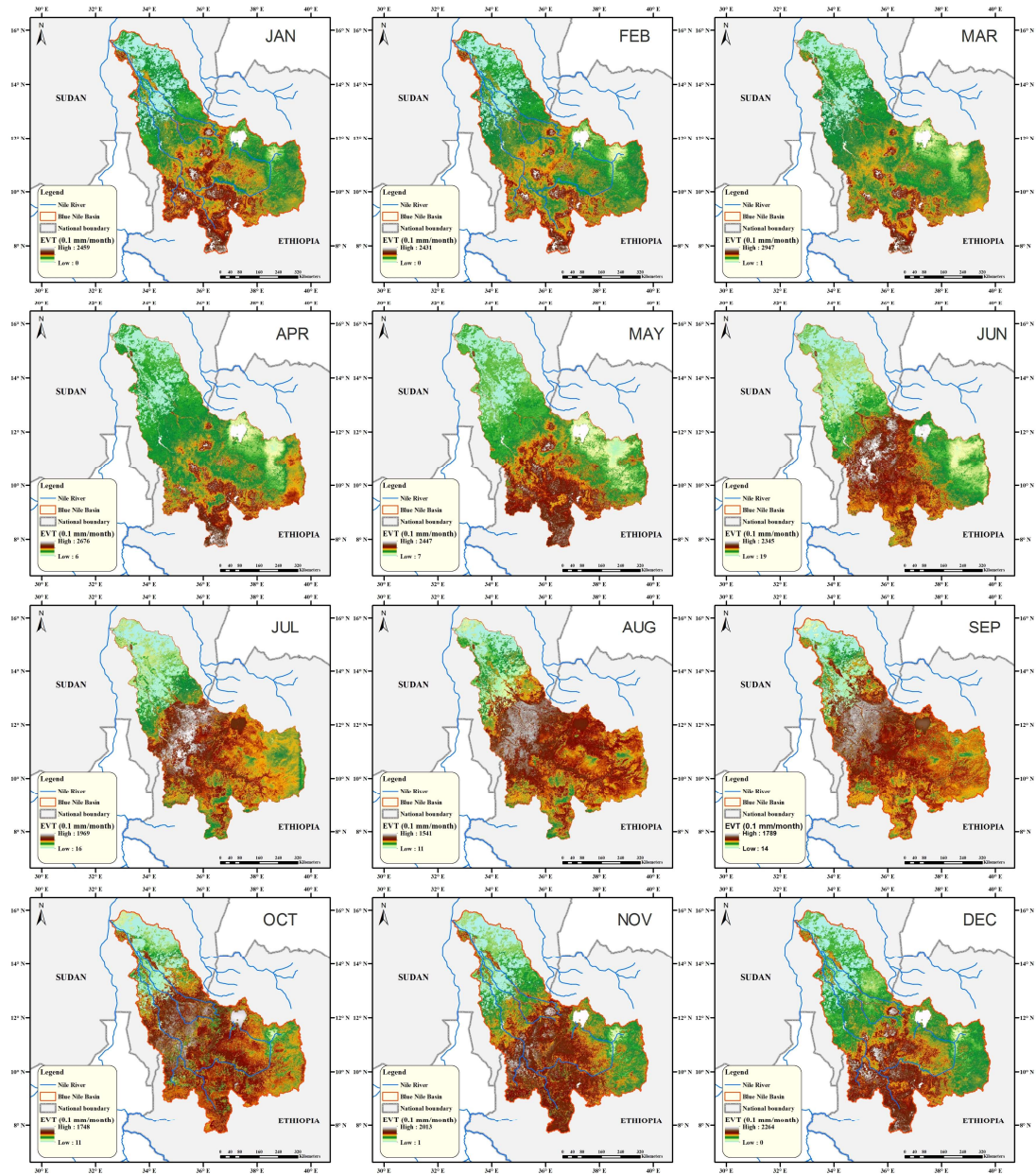


Figure 5 Average monthly evapotranspiration in the study area

4.1.2. Topography

Topographic data for the Blue Nile Basin have been acquired from the hole-filled Shuttle Radar Topography Mission (SRTM; Jarvis et al. (2008)). Figure 6 shows the topography of the Blue Nile Basin. SRTM provides digital elevation data for approximately 80% of the globe with a spatial resolution of 3 arc second (around 90 m × 90 m). It is worth noting that SRTM also provides topographic data at a 30 m spatial resolution; however, a 90 m resolution was used in this study to reduce data processing time. SRTM was initially

developed by The National Aeronautics and Space Administration (NASA) of the United States of America (USA). Then the product was further processed by a group of scientists to fill in the data gaps (Jarvis et al., 2008). SRTM data are available from 60 degrees north to 60 degrees south as 5-degree x 5-degree tiles in the WGS84 geographic coordinate system. The topographic data are added to the Blue Nile Basin database in a Raster (GeoTiff) format and has a unit of meters above sea level. The topographic data in the database have the same coordinate system as the parent data.

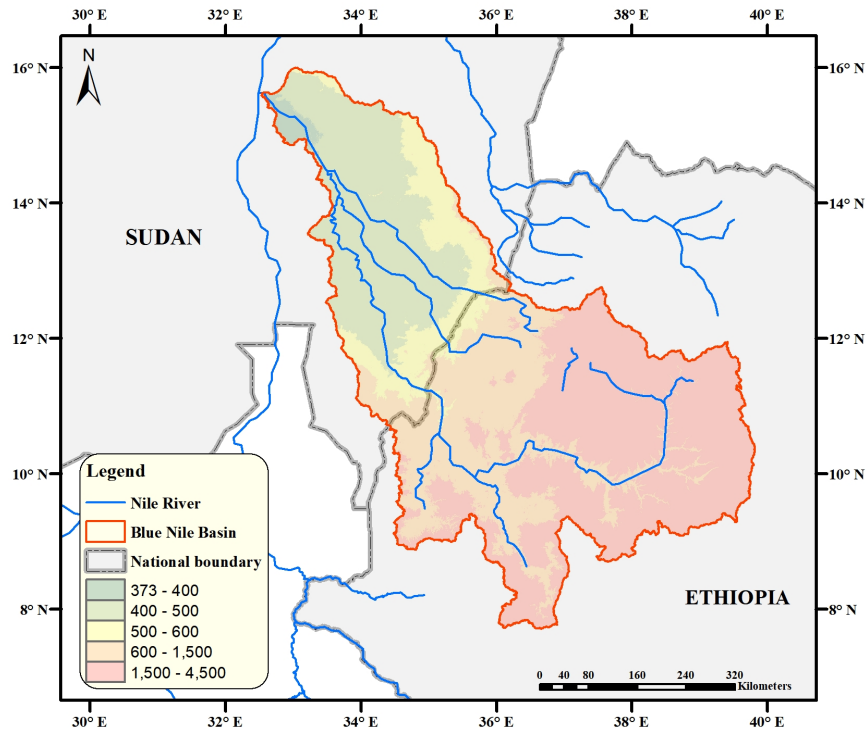


Figure 6 Topography of the study area

4.2. Descriptive data

This data category includes reservoir geometry, reservoir evaporation coefficients, and dam outlet specifications for the Grand Ethiopian Renaissance Dam (GERD), Roseires Dam, and Sennar Dam. It is worth noting that the GERD is currently under construction while Roseires and Sennar dams were constructed in 1966 and 1925, respectively.

4.2.1. Reservoir geometry

This sub-category of the database includes the geometry of the reservoirs of the GERD, Roseires Dam, and Sennar Dam (Figure 7). The geometry data consists of the elevation-volume table and the elevation-area table for each of the three reservoirs. The elevation-volume table is a relationship between the reservoir water elevation and the reservoir storage volume, whereas the elevation-area table is a relationship between the reservoir

water elevation and the area of the reservoir water surface. Both sets of data are essential for the operation of the three dams. For the GERD, the reservoir geometry data were acquired from the Eastern Nile Technical Regional Office of the Nile Basin Initiative. For Roseires and Sennar dams, the geometry data were obtained from the Ministry of Water Resources, Irrigation, and Electricity of Sudan. The geometry data of the GERD are based on a topographical survey for the reservoir area that has been conducted in 2011. Furthermore, the data for Roseires and Sennar are based on surveys for the two reservoirs in 2012 and 1985, respectively. The reservoir geometry data in the database are in Microsoft Excel format (.xlsx). The elevation is added in meters above sea level, the volume in million cubic meters, and the area in kilometres squared. The data for each reservoir is included in a separate Excel file, and the elevation-volume and the elevation-area tables are added to separate sheets.

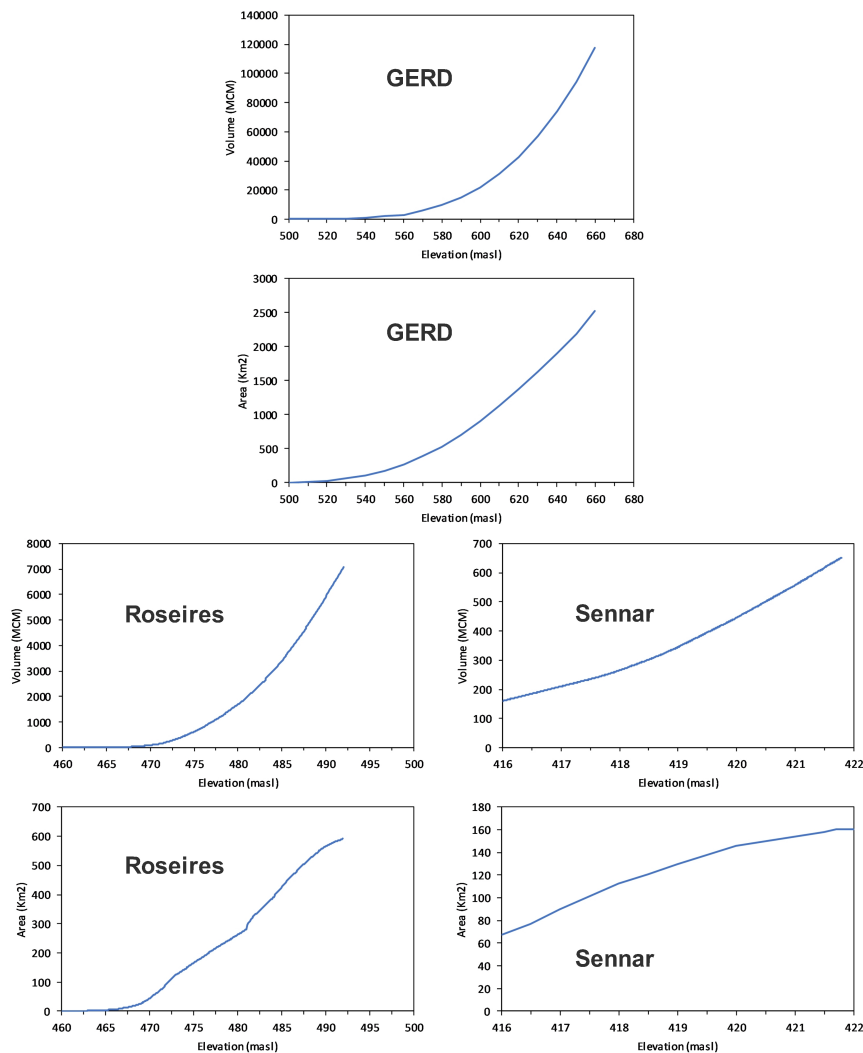


Figure 7 Geometry of the reservoirs in study area

4.2.2. Reservoir evaporation coefficients

Average monthly evaporation coefficients for each of the GERD, Roseires, and Sennar reservoirs are included in this sub-category of the Blue Nile database (Figure 8). For the GERD, the data have been acquired from Wheeler et al. (2016). The evaporation coefficients of Roseires and Sennar reservoirs were obtained from the Ministry of Water Resources, Irrigation, and Electricity of Sudan. GERD evaporation coefficients were derived in 2011 whereas as the evaporation coefficients of Roseires and Sennar reservoirs date back to 2012 and 1985, respectively. The data in the database are in Microsoft Excel format (.xlsx). The data for each reservoir are included in a separate file. As regards the unit, the data are provided in centimeters per month.

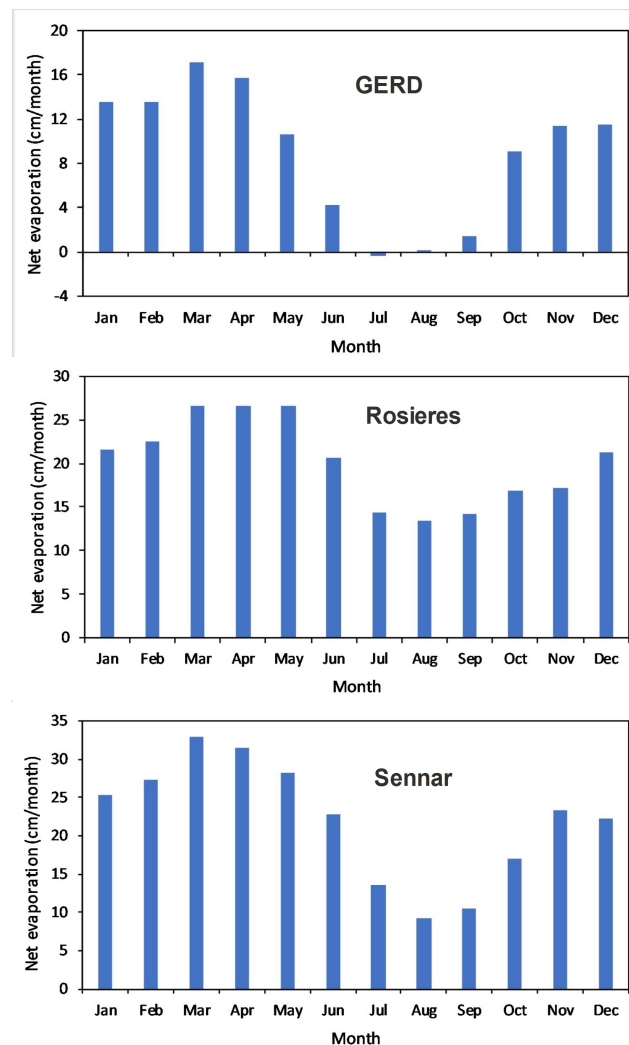


Figure 8 Net evaporation of the reservoirs in study area

4.2.3. Dam outlet specifications

This sub-category of the database includes the relationship between reservoir water level and physical water release capacity for each of the GERD, Roseires Dam, and Sennar Dam (Figure 9). The physical release capacity is the total amount of water that can be released through bottom outlets, turbines outlets, and spillways. This capacity is dependent on the available water head at any given time. The data for the three dams were collected from the Ministry of Water Resources, Irrigation, and Electricity of Sudan. The data for each of the three dams are included in the database in separate Excel files. The Excel files have a “.xlsx” format.

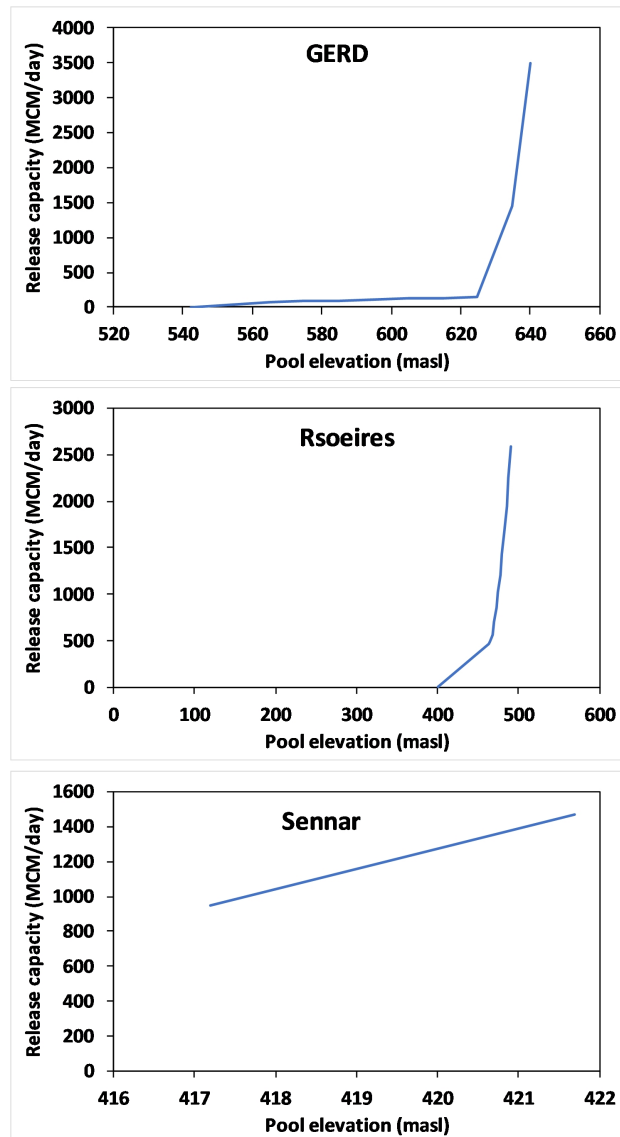


Figure 9 Total release capacity of the three dams in the study area

4.3. Geographic data

4.3.1. Existing and planned irrigation schemes

The Blue Nile Basin downstream the GERD includes several existing and planned irrigation schemes (Figure 3). The existing schemes include Gezira and Managil, Rahad 1, Suki, North West Sennar, and Gunied. On the other hands, the planned schemes are Kenana 1, Kenana 2, Kenana 3, Kenana 4, Roseires, Dinder South, Dinder North, Rahad 2 South, and Rahad 2 North. This section of the database includes the locations and extent of each of the existing and planned schemes in the study area. The polygons of the schemes are included in a single shapefile. The names of the schemes and their status (i.e. existing or planned) are included in the attribute table of the shapefile. The shapefile was zipped in “.7z” format before it was uploaded to the database. The shapefile is in the WGS84 geographic coordinate system. The source of the data is the Ministry of Water Resources, Irrigation, and Electricity of Sudan.

4.3.2. Hydraulic structures

The study area encompasses three dams (Figure 2): the GERD which is under construction since 2011; Roseires dam which was built in 1966; Sennar Dam which was constructed in 1925. The locations of the three dams are included in a shapefile which has been added to the database. The locations of the three dams were manually digitized utilizing Landsat satellite images from the United States Geological Survey (USGS) which is a scientific agency of the United States government. The attribute table of the shapefile includes the names of the three dams. The shapefile was zipped in “.7z” format before it was uploaded to the database. The shapefile is in the WGS84 geographic coordinate system.

4.3.3. River streams

Major river streams in the Blue Nile Basin were delineated based on the hole-filled Shuttle Radar Topography Mission (SRTM; see Section 4.1.2). Figure 6 shows the major river streams in the study area. HEC-GeoHMS, a tool developed by the Hydrologic Engineering Center of the USA Army Corps of Engineers, was used to perform the delineation of river streams in the Blue Nile Basin. The streams' data were prepared in a shapefile format and then zipped in “.7z” format before being uploaded to the database. The attribute table of the shapefile includes the names of the river streams downstream the GERD. The shapefile is in the WGS84 geographic coordinate system.

4.3.4. Natural reserves

The study area encompasses the Dinder National Park, a biosphere reserve located in Sudan (Figure 10). A shapefile of the extent and location of the park has been included in the database. The shapefile was zipped in “.7z” format before it was uploaded to the

database. The shapefile was acquired from Sulieman and Mohammed (2014) and is in the WGS84 geographic coordinate system.

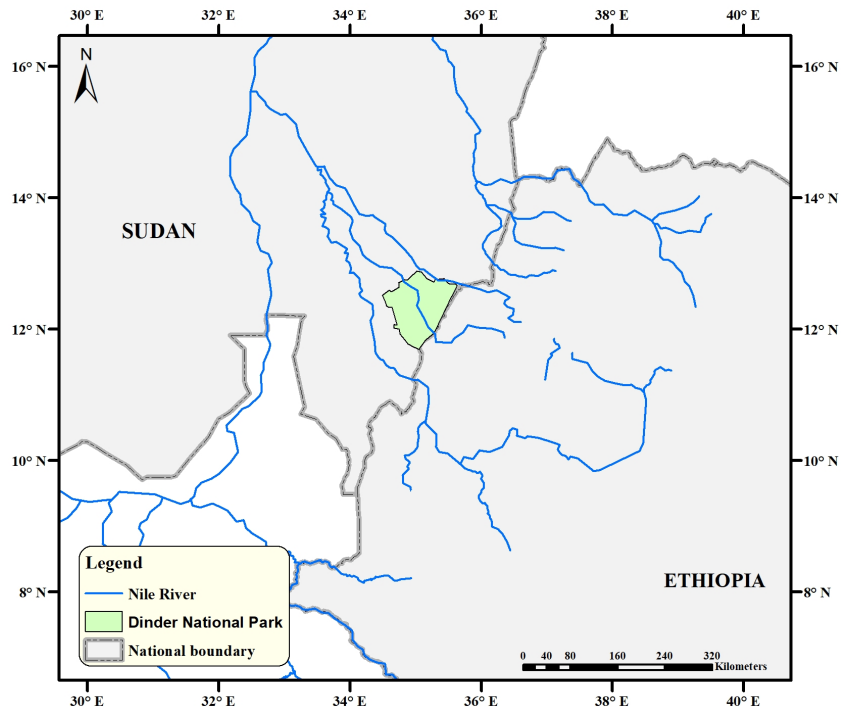


Figure 10 Location of the Dinder National Park

4.3.5. Weather and flow stations

The study area encompasses four stage-discharge stations, four stage stations, and five weather stations that are currently in operation (Figure 11). The stage-discharge stations report the Blue Nile discharge and water levels whereas the stage stations report water levels only. The weather stations report several climatic parameters such as rainfall, wind speed, sunshine hours, etc. The four stage-discharge stations are Eldiem, Khartoum, El-Guisi, and El-Hawata whereas the four stage stations include Wad-Elhadad, Hag Abdulla, Wad Medani, and El-Kamleen. Furthermore, the five weather stations are Damazine, Abu Na'ama, Sennar, El-Gedarif, Wad Medani, and Khartoum. The locations of the stations were added to a shapefile, zipped in “.7z” format, and then uploaded to the database. The attribute table of the shapefile includes the names and the types of the stations. The locations of the stage-discharge and stage stations were acquired from the Ministry of Water Resources, Irrigation, and Electricity of Sudan. The locations of the weather

stations were obtained from WMO (2016). The shapefile is in the WGS84 geographic

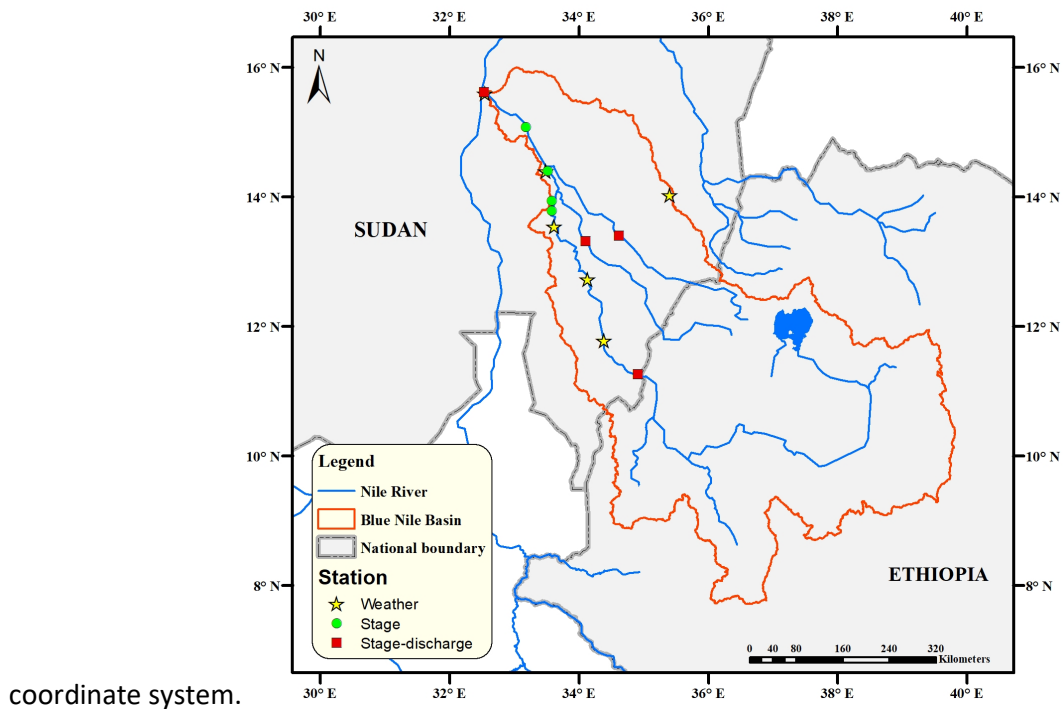


Figure 11 River and weather stations in the study area

4.4. Point data

4.4.1. Monthly rainfall

This sub-category includes monthly rainfall data for five ground weather stations, namely Damazine, Sennar, Wad Medani, Sennar, and El-Gedarif. The data covers the period from 1999 to 2009 (Figure 12). Raw daily rainfall time series of the five stations were purchased from Sudan Meteorological Authority and then aggregated into monthly data. Due to the data use policy of Sudan Meteorological Authority, we are unable to include the raw daily rainfall records in the database. However, we used the raw data as a comparison benchmark to evaluate the performance of long-term daily satellite-based rainfall products and to spot the best performing one in the study area. The monthly rainfall data are presented in the database in Microsoft Excel format “.xlsx” in a single workbook and a single sheet. The data unit is millimeters per month.

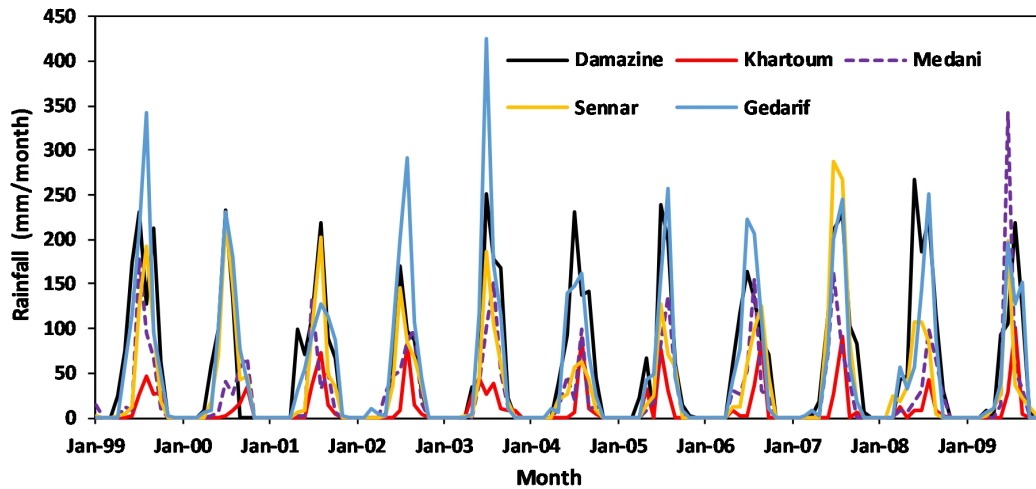


Figure 12 Average monthly rainfall at five stations in the study area

4.4.2. Average daily river flow

The database includes average daily river flow data for the four river discharge stations located in the study area. The stations are El-Diem, Khartoum, El-Guisi, and El-Hawata. Daily river flow time series for the four stations were obtained from the Ministry of Water Resources, Irrigation, and Electricity of Sudan for the period 1984 to 2016. For each of the four discharge stations, the time series were averaged to calculate the mean daily river flow data (Figure 13). Unfortunately, the raw daily time series cannot be included in the database due to the data use and distribution policy of the Ministry of Water Resources, Irrigation, and Electricity of Sudan. However, the raw data have been used in the modelling exercise. The average daily river flow data for 1984-2019 are presented in the database in Microsoft Excel format “.xlsx” in a single workbook and a single sheet. The data unit is million cubic meter month.

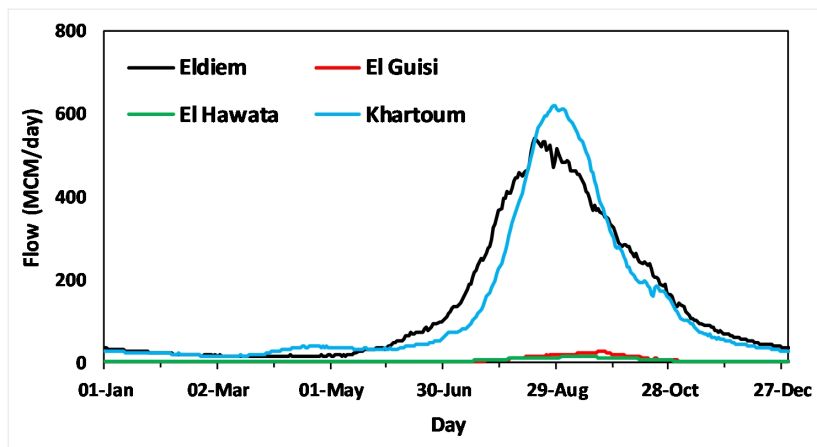


Figure 13 Average daily river flow at four stations in the study area

4.4.3. Average monthly water abstractions

This sub-category includes average monthly water abstractions by the major irrigation and domestic water users in the study area (Table 5). Five primary irrigation water users are located in the study area, i.e. Gezira and Managil, Rahad 1, Suki, North West Sennar, and Gunied, whereas only one weighty domestic water user is in the study area which is the City of Khartoum. Average monthly abstractions for the water users mentioned above were obtained from the Ministry of Water Resources, Irrigation, and Electricity of Sudan and added to the database. The average data are presented in the database in Microsoft Excel format “.xlsx” in a single workbook and a single sheet. The data unit is million cubic meter month.

Table 5 Major water abstraction in the study area

Month	Irrigation (MCM)					Domestic (MCM)
	Rahad1	Suki	Gezira and Managil	North-West Sennar	Gunied	Khartoum
Jan	90	58	660	21	23	0.01
Feb	77	47	548	23	18	0.01
Mar	31	42	440	23	20	0.01
Apr	15	45	61	27	23	0.01
May	81	41	139	31	22	0.01
Jun	141	37	364	29	30	0.01
Jul	134	88	708	25	23	0.01
Aug	19	42	450	22	9	0.01
Sep	68	48	709	26	37	0.01
Oct	177	100	873	31	28	0.01
Nov	108	89	803	36	28	0.01
Dec	101	77	719	28	27	0.01

5. Water-energy-food-ecosystem nexus modeling

5.1. Model components

A daily model was developed for the study area to simulate water allocation and rainfall-runoff of ungaged river streams. The model covers the 1984 to 2016 period. Several modeling tools were used in this study (see Section 5.2). Figure 14 shows a schematic of the model developed herein. The model includes three storage reservoirs (GERD, Roseires Dam, and Sennar Dam), seven inflow nodes, five irrigation demand nodes, evaporation losses from the storage reservoirs, return flows from irrigation schemes, and transmission losses (i.e. channel evaporation and percolation) from river reaches. The model is driven by the inflows from the Blue Nile, Dinder, Rahad, and Sub-basins 1-5. Moreover, outflow from the storage reservoirs was calculated based on their operating rules. These rules were obtained from Basheer et al. (2018). River flow data from El-Gewisi, EL-Hawata, and EL-Diem stations were used as inflows for the Dinder, Rahad, and the Blue Nile respectively. The rainfall-runoff component of the model was used to simulate the inflow from Sub-basins 1 to 5 because they are ungaged. Due to the scarcity of ground rainfall stations in the study area, the performance of satellite-based rainfall products was evaluated and the best performing one was used as a boundary condition to the rainfall-runoff component of the model. Section 5.3 explains the methods used to evaluate the satellite rainfall data and performance results.

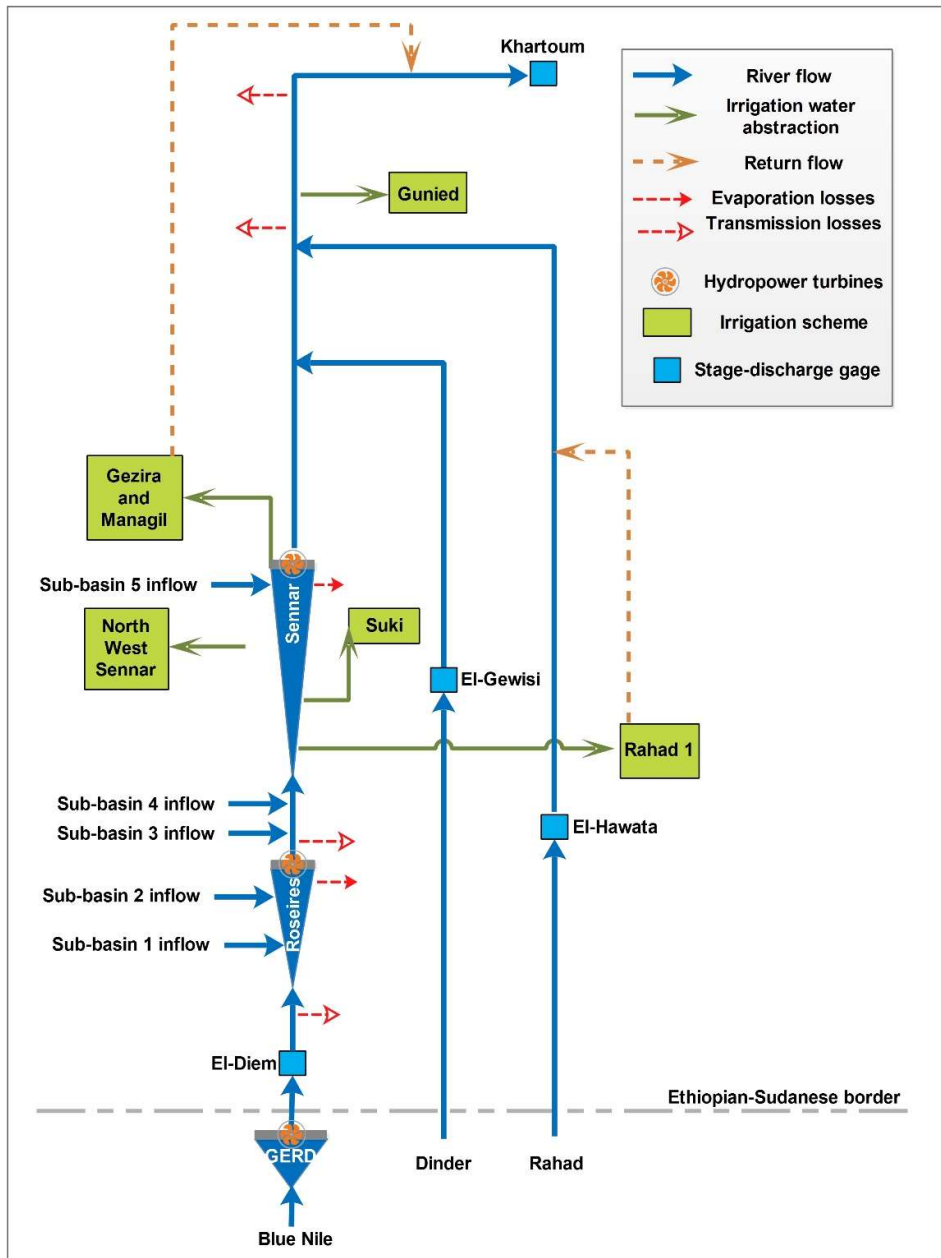


Figure 14 Schematic of the water balance model

5.2. Modeling framework

Figure 15 shows the modeling framework of this study. Water allocation in the study area was simulated using RiverWare, which is a general river and reservoir simulation software developed by the University of Colorado Boulder (Zagona et al., 2001). With a time step ranging from one hour to one year, RiverWare is capable of simulating hydraulic and hydrologic processes of reservoirs, river reaches, diversions, canals, abstractions, groundwater interaction, hydropower production, water ownership, and water accounting

transactions. All the previously mentioned simulation capabilities proved to be useful in operation scheduling, planning, and policy evaluation (Basheer et al., 2019, 2018; Wheeler et al., 2016; Zagona et al., 2008). The object-oriented approach of RiverWare allows the user to create a network of objects, link them, populate each one with data, and select the appropriate physical process (Zagona et al., 2008). Moreover, the Rule-based simulation, which RiverWare supports, gives the ability to simulate operation policies using logical policy statements rather than explicitly specified input values for operations. This ability provides high flexibility in simulating complex river systems. Additionally, RiverWare includes an important utility called Multiple Run Management through which the user can run a model using traces of stochastically generated hydrologic inputs. RiverWare has appeared to be successful in its recent use in the transboundary negotiations over the Colorado River and modeling the Eastern Nile Basin (Basheer et al., 2018; Basheer and Elagib, 2018a; Wheeler et al., 2016).

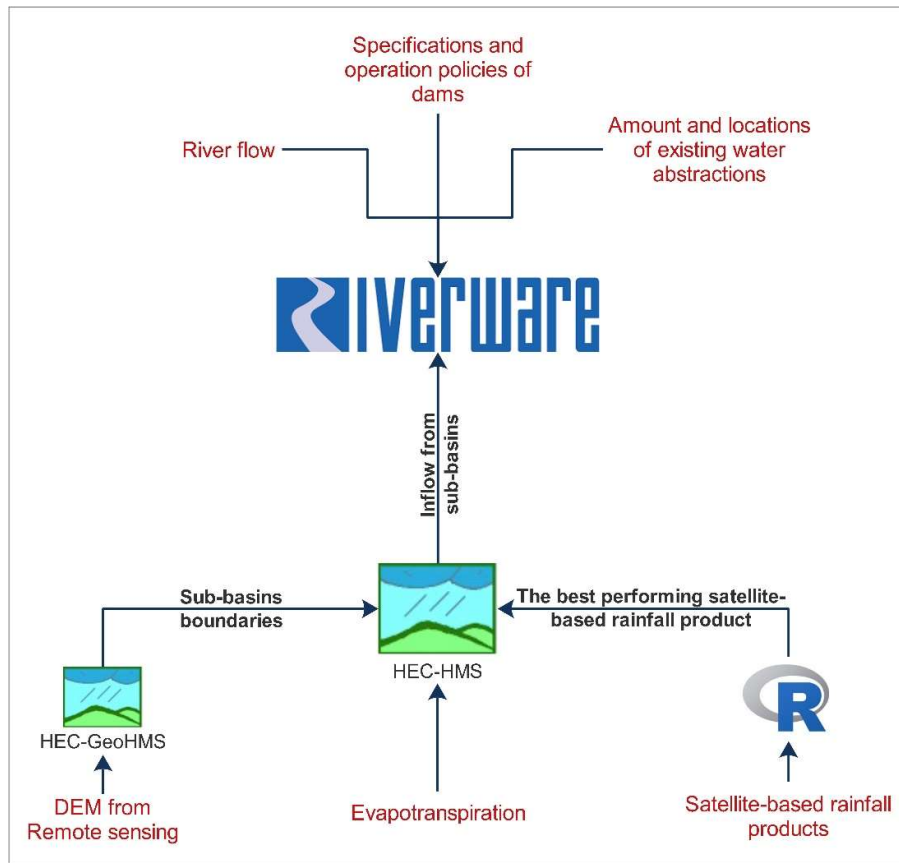


Figure 15 Modeling framework used in this study

HEC-HMS was used to simulate the hydrological processes. HEC-HMS, developed by the Hydrologic Engineering Centre, is a freely accessible numerical model (computer program) that includes a large set of methods to simulate rainfall-runoff for dendritic watershed

systems. HEC-HMS simulates watershed precipitation and evaporation, runoff volume, direct runoff, baseflow, and channel flow (HEC, 2008). HEC-GeoHMS was used to visualize spatial information, document watershed characteristics, perform spatial analysis, delineate sub-basins and streams, and construct inputs to HEC-HMS (Asadi and Boustani, 2013; HEC, 2009). Table 6 shows the methods used to simulate the different hydrological processes.

R, an open source programming language, was used in evaluating the performance of satellite-based rainfall products. R provides several packages and functions that are capable of downloading remote sensing data, extracting pixel values, and calculating the average of pixels within sub-basins (R Core Team, 2015).

Table 6 Methods used for simulating various processes

Process	Method
Runoff volume	Deficit and constant loss
Direct runoff	Snyder’s unit hydrograph
Baseflow	Monthly-Varying Baseflow
Flow routing	Lag time
Canopy interception	Simple canopy
Transmission losses	Percentage loss
Reservoir evaporation	Average monthly rate
Surface evapotranspiration	Average monthly

5.3. Evaluation of satellite-based rainfall products

Due to the limited number of available rainfall gauges in the study area, four satellite-based rainfall products have been evaluated and the best performing one was used as a boundary condition to model rainfall-runoff in the study area. The evaluated satellite-based rainfall products include the African Rainfall Climatology Version 2 (ARC2.0; Novella and Thiaw, (2013)), Tropical Applications of Meteorology Using Satellite Data and Ground-Based Observations version 2 (TAMSAT2; Maidment et al. (2014)), Precipitation Estimation from Remotely Sensed Information Using Artificial Neural Networks–Climate Data Record (PERSIANN-CDR; Ashouri et al. (2015)), and Climate Hazards group Infrared Precipitation with Stations version 2.0 (CHIRPS 2.0; Funk et al. (2014)).

To measure the difference between satellite estimates and ground observations, a pixel-to-point evaluation was conducted for the satellite products at the locations of five ground rainfall stations using the available measured data (1999 to 2009). Figure 16 shows the locations of the five ground stations. Six performance metrics were used to conduct

the evaluation. Those metrics can be categorized into two groups: (1) error metrics that include the root mean square error (RMSE; Chai and Draxler (2014)), the mean bias error (MBE; Legates and McCabe Jr (1999)), and the coefficient of determination (R^2 ; Legates and McCabe Jr (1999)) (2) categorical metrics that include the probability of detection (POD; Toté et al. (2015)), the false alarm ratio (FAR; Diem et al. (2014)), and the equitable threat score (ETS; Ebert et al. (2007)). Equations 1 to 6 shows the performance metrics used in evaluating the performance of the four satellite-based rainfall products.

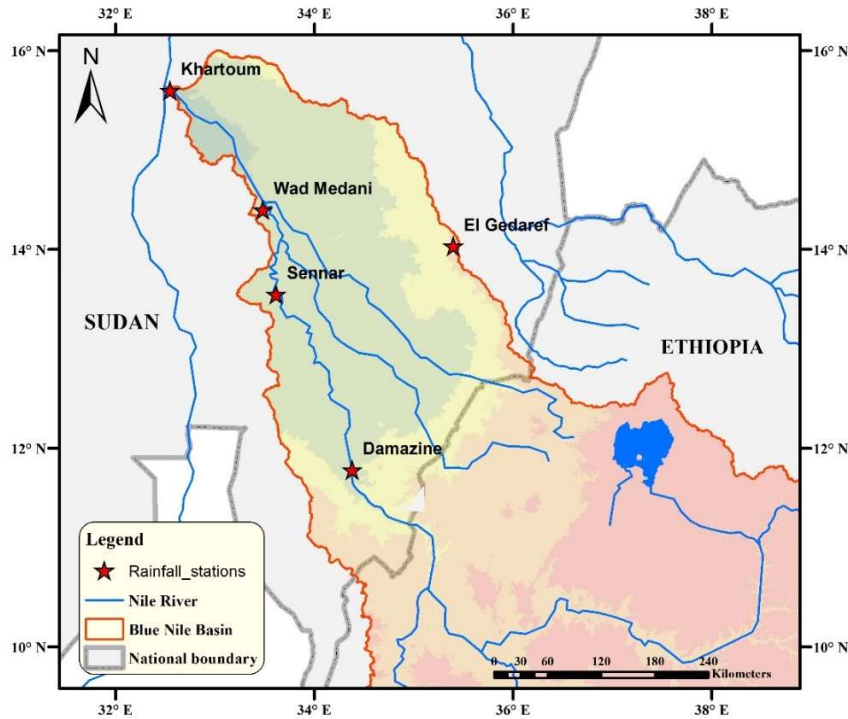


Figure 16 Rainfall stations used in this study

In order to calculate any of the categorical metrics, a threshold of 0.1 mm per day will be used to classify each time step within the evaluation period into a hit (h) when rainfall was both observed by the gauge and estimated by the satellite-based rainfall product; a miss (m) when rainfall is observed by the gauge but not estimated by the satellite-based rainfall product; a false alarm (f) when rainfall was estimated by the satellite-based rainfall product but not observed by the gauge; or null (n) when rainfall was neither observed by the gauge nor estimated by the satellite-based rainfall product (Diem et al., 2014; Ebert et al., 2007; Zambrano-Bigiarini et al., 2017).

$$RMSE(mm) = \sqrt{\frac{1}{n} \sum_{i=1}^n (S_i - G_i)^2} \quad (1)$$

$$MBE(mm) = \frac{1}{n} \sum_{i=1}^n (S_i - G_i) \quad (2)$$

$$R^2 = \frac{(n(\sum_{i=1}^n G_i S_i) - (\sum_{i=1}^n G_i)(\sum_{i=1}^n S_i))^2}{(n(\sum_{i=1}^n G_i^2) - (\sum_{i=1}^n G_i)^2)(n(\sum_{i=1}^n S_i^2) - (\sum_{i=1}^n S_i)^2)} \quad (3)$$

$$POD = \frac{H}{H+M} \quad (4)$$

$$FAR = \frac{F}{H+F} \quad (5)$$

$$ETS = \frac{H-H_e}{H+M+F-H_e} \quad (6)$$

$$H_e = \frac{(H+M)(H+F)}{N} \quad (7)$$

Where:

G_i = the i^{th} Gauge observation (mm)

S_i = the i^{th} Satellite rainfall estimate (mm)

n = number of data pairs

\bar{G} = the mean of the Gauge observations (mm)

H = total number of Hits

M = total number of Misses

F = total number of False alarms

N = total number of Nulls

H_e = the number of Hits due to random chance

Figure 17 shows the performance metrics of the four satellite-based rainfall products at five locations. It is evident in the figure that the ARC2 has the best performance in terms of ETS, R^2 , RMSE, and FAR at all locations compared to the other rainfall products. Furthermore, ARC2 has the second best performance in terms of POD and MBE. In order to draw an overall conclusion on the best performing product based on all performance metrics, the overall unified metric (OUM) was calculated for each of the evaluated satellite-based rainfall products. OUM is a performance metric developed by Basheer and Elagib (2018b) based on summing up the performance rankings. Equations 8 and 9 below show the calculation procedure. High OUM values indicate poor performance and vice versa. We refer the reader to Basheer and Elagib (2018b) for further information.

$$UM_{rj} = \sum_{i=1}^p R_{rji} \quad (8)$$

$$OUM_r = \sum_{j=1}^e UM_{rj} \quad (9)$$

Where:

UM_{rj} = the Unified Metric of the rainfall product r at the station j

p = the number of performance metrics

R_{rji} = the performance ranking of the rainfall product r —compared to the other products—
at the station j based on the performance metric i

OUM_r = the Overall Unified Metric of the rainfall product r

e = the number of stations

UM_{rj} = the Unified Metric of the rainfall product r at the station j

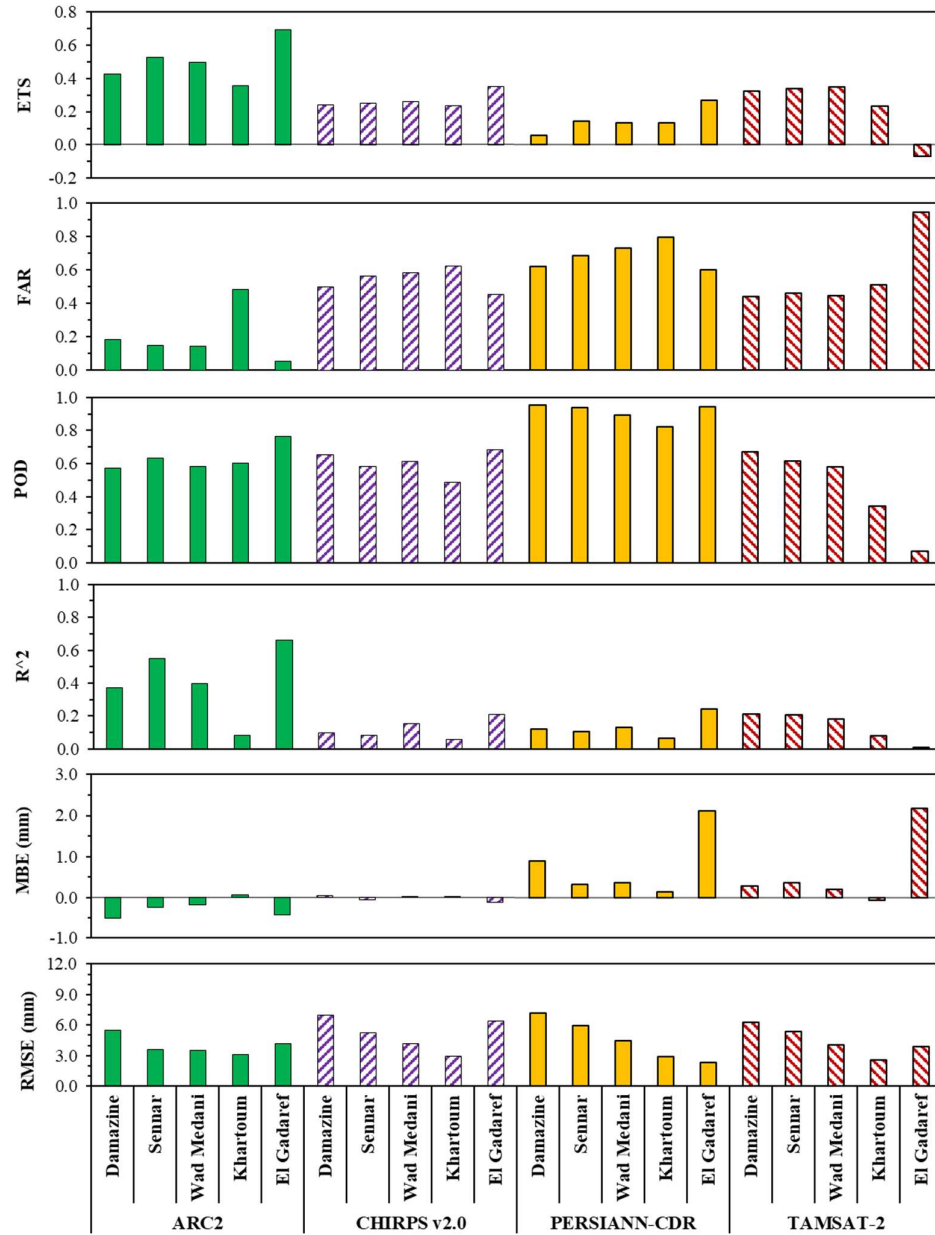


Figure 17 Performance metrics of the evaluated satellite-based rainfall products

Figure 18 shows the overall unified metric of the four satellite-based rainfall products that have been evaluated in this study. The figure shows that ARC2 outperformed the other satellite-based rainfall products at all evaluation locations. Therefore, ARC2 has been used as a boundary condition to model rainfall-runoff in the study area.

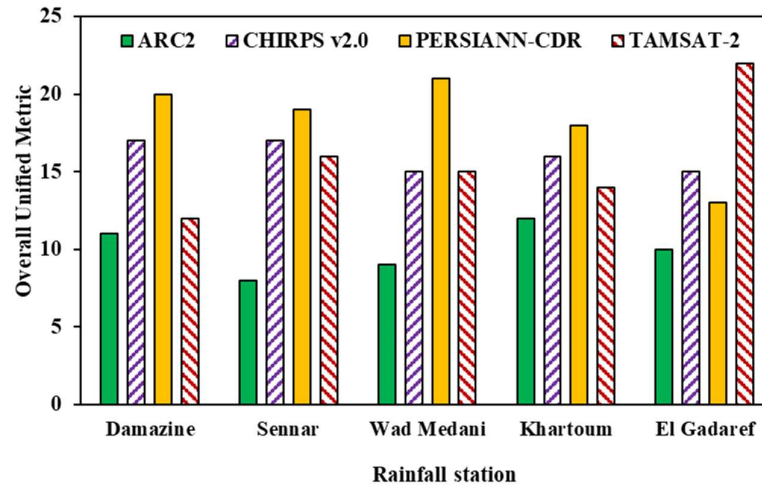


Figure 18 Overall performance of the satellite-based rainfall products in the study area

5.4. Model performance

The model performance was assessed according to the recommendations of Stern et al. (2016) which provided performance ranking for daily models based on a quantitative comparison of simulated and observed flow values using three statistical performance metrics. The three metrics include the coefficient of determination (R^2), Nash–Sutcliffe Efficiency (NSE), and the Mean Error Percentage (MPE). Equations 10, 11, and 12 were used to calculate the three statistical metrics. R^2 ranges from zero to one, with higher values demonstrating better performance.. NSE can take any value from one to $-\infty$ with one indicating perfect prediction ability, zero indicating that the prediction of the model is as good as the average of the observed data, and negative values showing that the average of the observed data is better than the model prediction. Lastly, the Mean Error Percentage (MEP) ranges from -100 to $+\infty$ with values closer to zero indicating better performance.

The performance of the model was assessed using river discharge at three locations: the Rosieres Dam, the Sennar Dam, and the Khartoum Gage. The model was calibrated from 1984 to 2000 and validated from 2001 to 2016. The calibration parameters include soil infiltration rate, maximum soil storage capacity, time of concentration of sub-basins, Snyder peaking coefficient, lag times, canopy interception, and transmission losses.

$$R^2 = \frac{\left(n \left(\sum_{i=1}^n Y_i^{obs} Y_i^{sim} \right) - \left(\sum_{i=1}^n Y_i^{obs} \right) \left(\sum_{i=1}^n Y_i^{sim} \right) \right)^2}{\left(n \left(\sum_{i=1}^n Y_i^{obs^2} \right) - \left(\sum_{i=1}^n Y_i^{obs} \right)^2 \right) \left(n \left(\sum_{i=1}^n Y_i^{sim^2} \right) - \left(\sum_{i=1}^n Y_i^{sim} \right)^2 \right)} \quad (10)$$

$$NSE = 1 - \frac{\sum_{i=1}^n (Y_i^{obs} - Y_i^{sim})^2}{\sum_{i=1}^n (Y_i^{obs} - Y_{mean})^2} \quad (11)$$

$$MEP = \frac{1}{n} \sum_{i=1}^n \frac{(Y_i^{obs} - Y_i^{sim})}{Y_i^{sim}} \times 100 \quad (12)$$

Where:

Y_i^{obs} = the i^{th} observed flow

Y_i^{sim} = the i^{th} simulated flow

n = number of data pairs

Figures 19 to 21 show the daily observed and simulated flows at the Roseires and Sennar dams and the Khartoum Gage. The figures show that the model could accurately capture the inter- and intra annual behavior of the Blue Nile. The high R^2 values show that a large portion of the variation in the observed flow could be explained by the variation in the simulated flow. Generally, the model showed better performance in the calibration period than in the validation period. This is because the operation of the Roseires Dam has not been fixed since the heightening of the dam in 2013. Table 7 shows the performance metrics and performance ranking. The model showed a predominantly excellent performance in the calibration and validation periods.

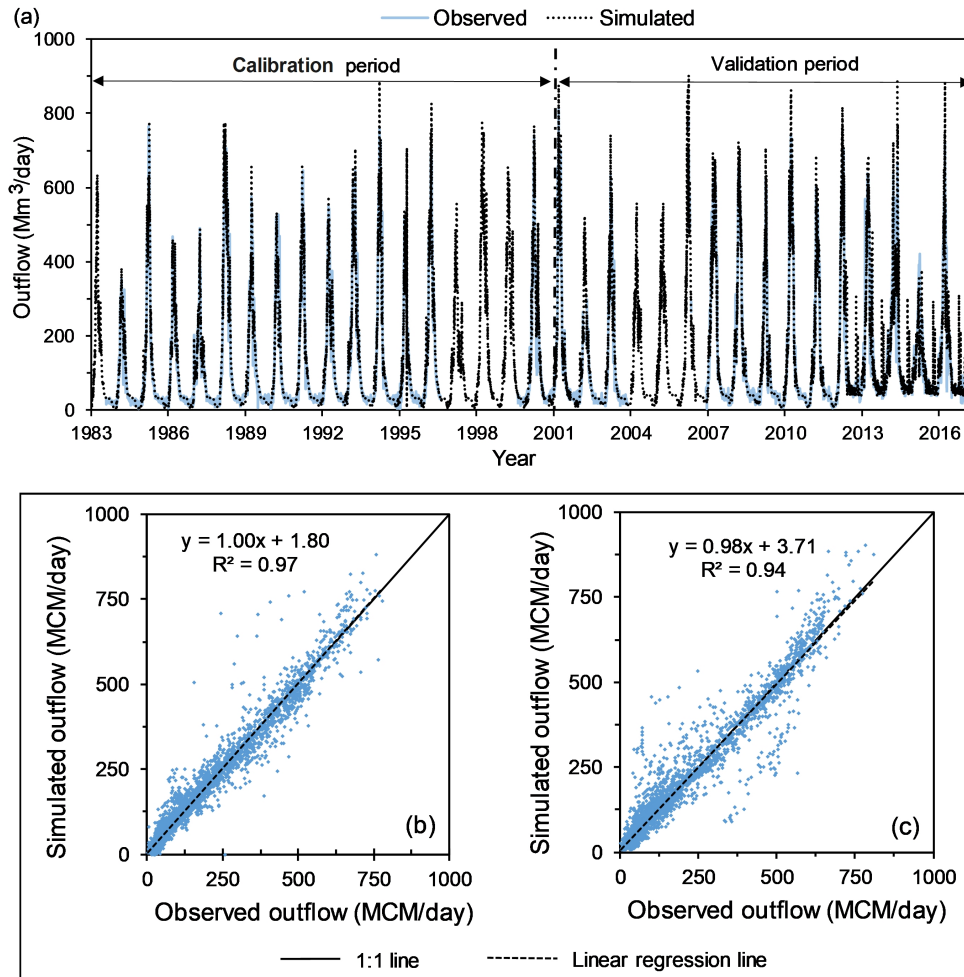


Figure 19 Daily observed and simulated outflow from the Roseires Dam: (a) time series for the calibration and validation periods (b) scatter plot of the calibration period, and (c) scatterplot of the validation period.

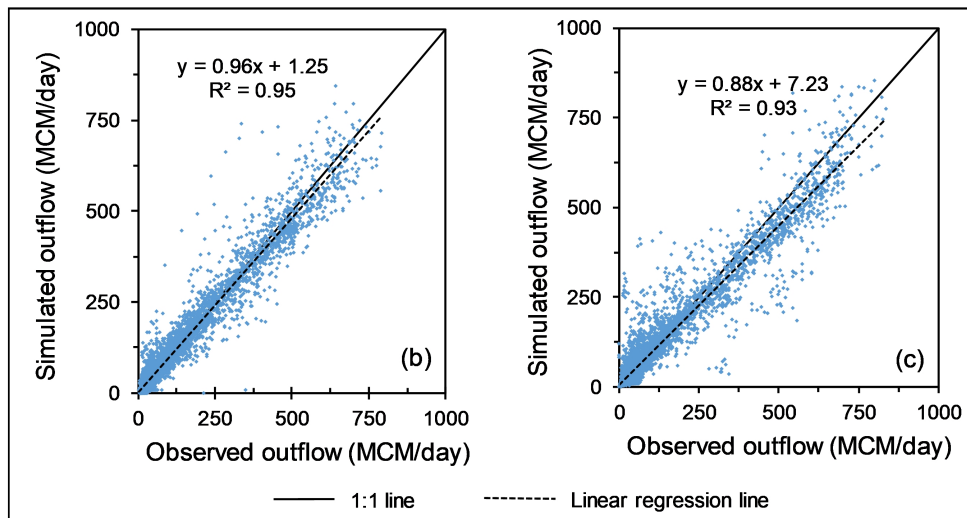
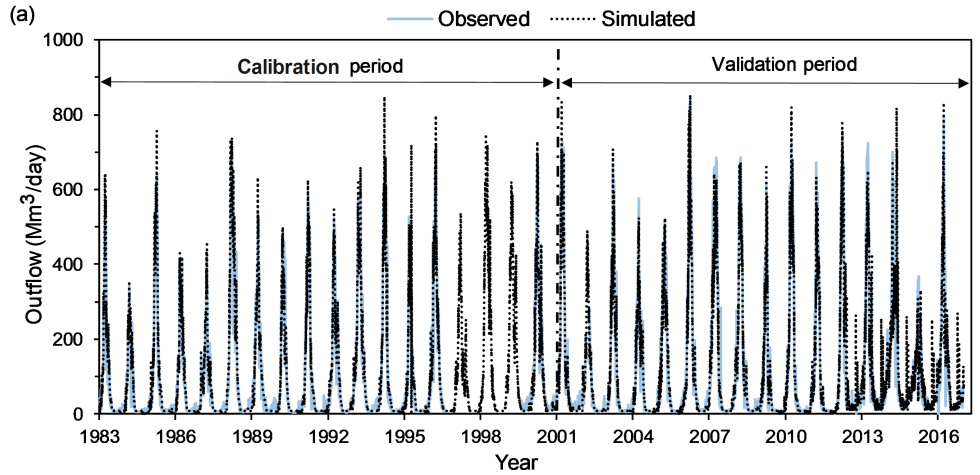


Figure 20 Daily observed and simulated outflow from the Sennar Dam: (a) time series for the calibration and validation periods (b) scatter plot of the calibration period, and (c) scatterplot of the validation period.

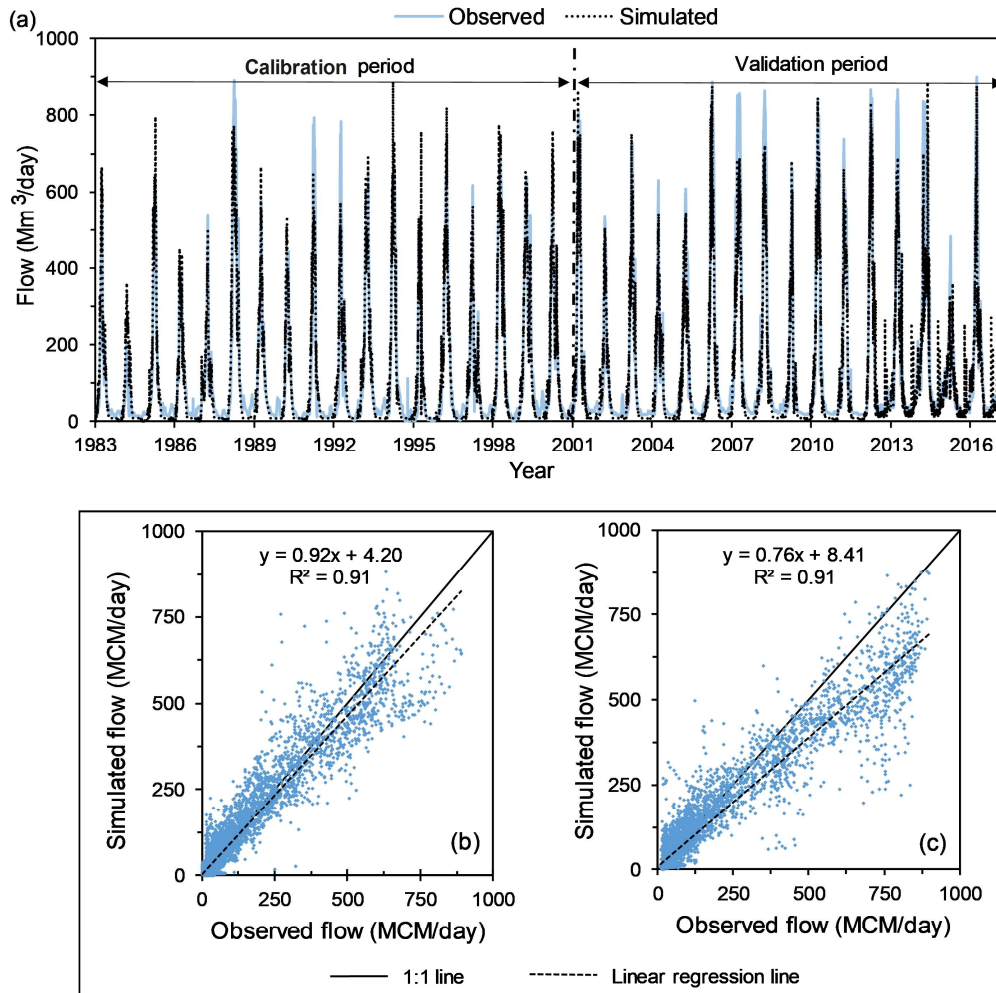


Figure 21 Daily observed and simulated flow at the Khartoum Gage: (a) time series for the calibration and validation periods (b) scatter plot of the calibration period, and (c) scatterplot of the validation period.

Table 7 Model performance at three locations in the study area

Location	Performance metric	Calibration		Validation	
		Metric value	Ranking	Metric value	Ranking
Rosieres Dam	R ²	0.97	Excellent	0.94	Excellent
	NSE	0.96	Excellent	0.98	Excellent
	MPE	0.88	Excellent	0.84	Excellent
Sennar Dam	R ²	0.95	Excellent	0.93	Excellent
	NSE	0.95	Excellent	0.96	Excellent
	MPE	-1.30	Excellent	8.95	Excellent
Khartoum Gage	R ²	0.90	Excellent	0.91	Excellent
	NSE	0.90	Excellent	0.92	Excellent
	MPE	0.26	Excellent	-13.08	Very good

5.5. Simulation scenarios

In this study, 34 simulation scenarios were examined. Figure 22 shows a flowchart of the scenarios. The examined scenarios comprise of a historic baseline scenario for the 1984-2016 period and a scenario with the GERD (in steady-state operation) on the river system. The latter scenario was examined across 33 hydrologic conditions (each 33 years long). The hydrologic conditions were developed using the index-sequential method (Kendall and Dracup, 1991; Ouarda et al., 1997). The index-sequential method is a technique that uses the historic flow record to generate synthetic hydrologic traces taking all years in the record as a possible starting point. This method was used because it requires minimal assumptions and inputs. Moreover, it preserves any serial correlation in the historic record.

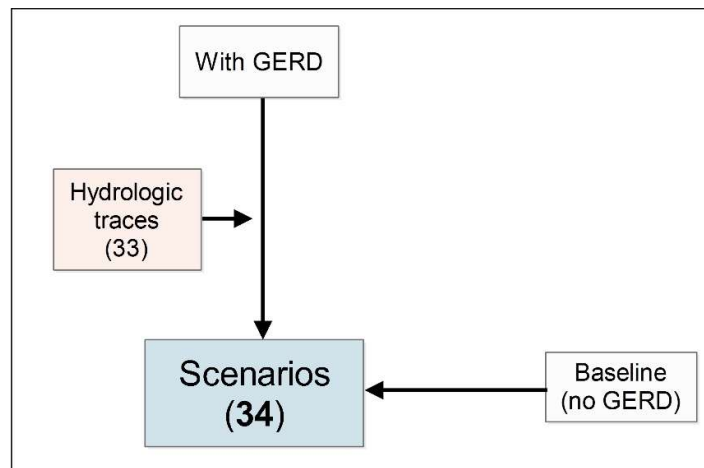


Figure 22 Scenarios modeled in this study

In the 33 scenarios that include the GERD in full operation, the operation of the Roseires and Sennar Dams was modified to keep them at their full supply level. This modification has been recommended by several studies (Basheer et al., 2018; Wheeler et al., 2018, 2016) to eliminate any water supply shortages in Sudan that would result for the regulation of the Blue Nile flow by the GERD. In this study, the GERD was assumed to target a power rate of 1,400 MW. Wheeler et al. (2018) found that this power rate would maximize the firm annual energy generation of the dam.

6. Water-energy-food-ecosystem nexus assessment

6.1. River flow

The standardized streamflow index was used to analyze the inter-annual variation of river flow in terms of deviation from the long-term mean. The standardized streamflow index (Modarres, 2007) is the deviation from the mean divided by the standard deviation. The standardized streamflow index was selected herein due to the near-normal distribution of the annual flow data of the Blue Nile judging by a skewness of around 0.15. Equation 13 was used to calculate the standardized streamflow index.

$$SSFI_i = \frac{F_i - \bar{F}}{\sigma} \quad (13)$$

Where:

SSFI = standardized streamflow index of the i^{th} year

F_i = the annual flow in the i^{th} year

\bar{F} = the mean of the annual flow time series

σ = the standard deviation of the annual flow time series

Figure 23 shows the standardized streamflow index of the Blue Nile flow at Eldiem near the Ethiopian-Sudanese border. The figure shows successive below-average years in the 1980s and the 1990s. These negative anomalies can be attributed to concurrent metrological droughts that hit Ethiopia and Sudan (Zhang et al., 2012). The time series of the standardized streamflow index shows a decrease in the length and severity of hydrological droughts in the 2000s. This change is due to an increase in rainfall and land cover changes in the Ethiopian highlands (Woldesenbet et al., 2017).

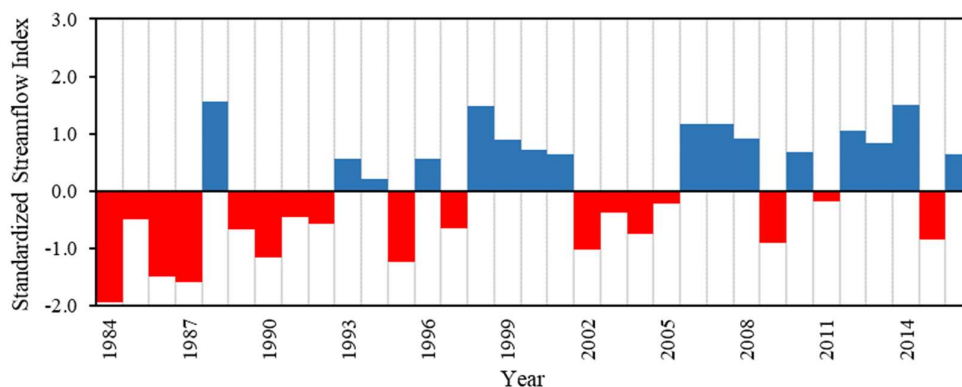


Figure 23 Historic standardized streamflow index of the Blue Nile at the Eldiem gage.

Figure 24 shows the probability of exceedance of the annual flow of the Blue Nile at Eldiem with and without the GERD. The figure shows that the steady-state operation of the GERD would reduce the inter-annual variability of the flow as explained by a reduction in the maximum annual flow and an increase in the minimum annual flow compared with the baseline. The decrease in variability would positively affect water availability in the Lower Blue Nile Basin. However, it implies a negative impact on recession agriculture along the Blue Nile.

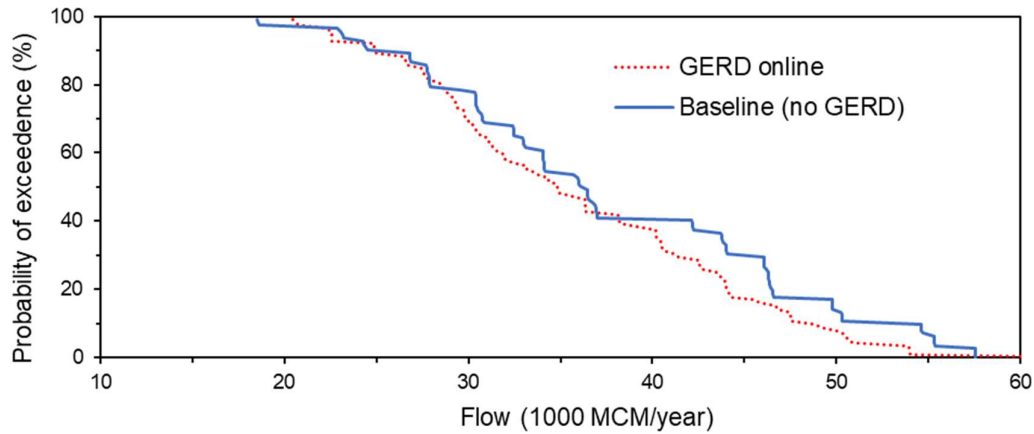


Figure 24 Exceedance probability of the Blue Nile flow at Eldiem with and without the GERD.

6.2. Energy generation and water-energy productivity

In this study, we used the annual energy generation and the annual water-energy productivity (WEP) as indicators for hydropower generation in the study area. The WEP is a water-energy nexus indicator developed by Basheer and Elagib (2018a). The WEP is the amount of energy produced per unit of water lost in the process. It is calculated annually for hydropower generation by dividing the total annual energy generation by the total annual evaporation losses. Equation 14 was used to calculate the WEP.

$$WEP_i = \frac{E_i}{EV_i} \quad (14)$$

Where:

WEP_i = is the water-energy productivity in the i^{th} year

E_i = the annual energy generation in the i^{th} year

EV_i = the annual reservoir evaporation in the i^{th} year

Figure 25 depicts the WEFE nexus indicators of the Blue Nile. The colors in the figure distinguish the years with high and low water-energy productivity. The figure shows a

historic annual energy generation in the study area in the range of around 1450 to 2410 GWh. The WEP took a range of 1775 to 2968 GWh/BCM from 1984 to 2016. Figure 25 shows that most of the years with the highest annual energy generation and low WEP are after 2012. This can be associated with the heightening of the Roseires Dam in 2013. This heightening increased both energy generation and reservoir evaporation, with a higher increase in the latter than in the former resulting in a decrease in the WEP. The WEP can be increased for the Roseires Dam by utilizing the increase in hydropower potential that resulted from the heightening. Hydropower turbines with a high capacity could be installed in the Roseires Dam to achieve that. Operating the reservoir at lower level could also be used to reduce the WEP; however this will result in water supply shortages bearing in mind that hydropower generation is not the primary purpose of the dam.

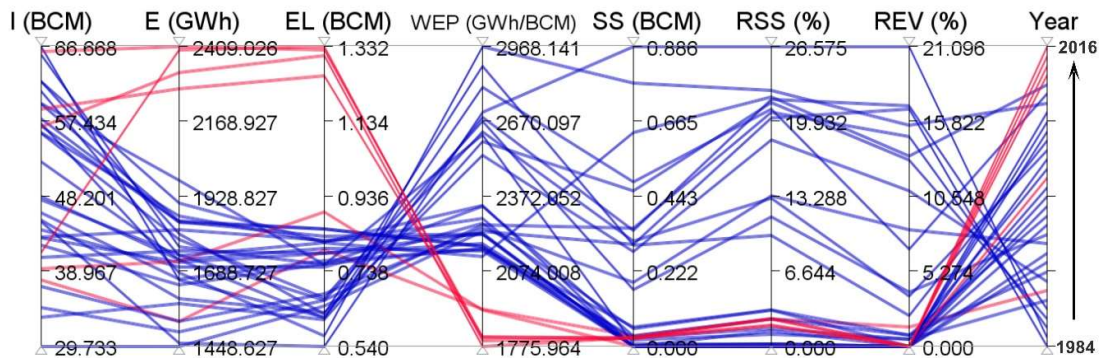


Figure 25 Parallel plots of the historic annual (1984-2016) water-energy-food-ecosystem nexus indicators.

Note: Blue- and red-colored lines represent years with high and low Water-Energy Productivity (WEP), respectively; I = inflow; E = energy generation; EL = evaporation losses; WEP = water-energy productivity; SS = irrigation supply shortages; RSS = risk of irrigation supply shortage; REV = risk to environmental flow violation.

The analysis of hydro-energy generation and reservoir evaporation in Sudan during the steady-state operation of the GERD reveals the following with all hydrologic conditions: a total annual energy generation for the Roseires and Sennar Dams of around 2560 GWh, a total annual evaporation from the Roseires and Sennar Dams of around 1.735 BCM, and a WEP of around 1575 GWh/BCM. These results indicate that the GERD would further decrease the WEP in Sudan due to an increase in reservoir evaporation at a faster rate than energy generation. Increasing the WEP would require utilizing the untapped hydropower potential from the Roseires and Sennar dams that the GERD would provide as a result of less inter-annual variability in river flow.

Figure 26 shows the exceedance probability of the steady-state annual energy generation from the GERD. The figure shows that energy generation from the GERD would

range between around 13000 and 20300 GWh per year. This represents a substantial increase in energy generation in the region that would hopefully stimulate energy trade and open venues for the economic development of Ethiopia and East Africa.

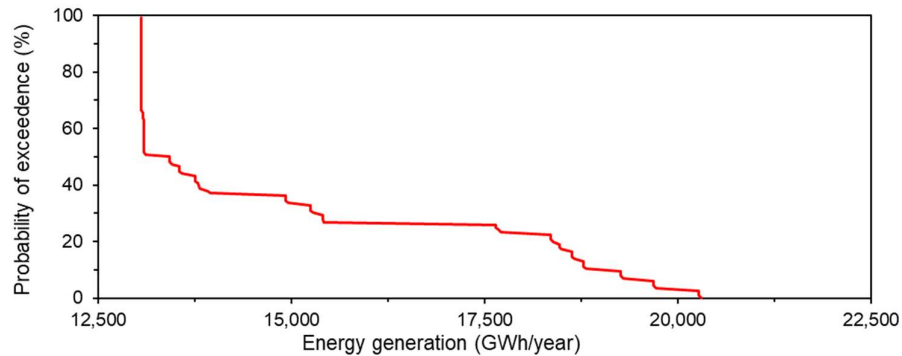


Figure 26 Steady-state energy generation from the Grand Ethiopian Renaissance Dam

6.3. Irrigation water supply

The annual irrigation water supply shortage (SS) and the risk of irrigation water supply shortage (RSS) have been used in this study as indicators of water-food nexus. The RSS is defined by Wheeler et al. (2016) as the percentage of days in the year with supply shortages. Equation 15 was used to calculate the RSS.

$$RSS = \frac{D}{DY} \times 100\% \quad (15)$$

Where:

RSS = is the risk of irrigation water supply shortage in the i^{th} year (%)

D = the number of days with irrigation water supply shortage in the i^{th} year

DY = the number of days in the i^{th} year

Figure 27 displays the historic WEFE nexus indicators for the study area. The figure shows that from 1984 to 2016, the annual irrigation water supply shortage and the annual risk of irrigation water supply shortage ranged from 0 to 0.886 BCM and 0 to 27%, respectively. High association is evident between the annual irrigation water supply shortages (SS), risk of supply shortages (RSS), and river flow (I). The highest shortages and risk occurred in the year 1985 during the drought of the 1980s and 1990s. The Blue lines in Figure 27 indicate the instances with low irrigation shortages. It can be noticed that the years with above-normal flow conditions (see Figure 23) often have low irrigation shortages. Moreover, low shortages were found from the year 2013 due to the heightening of the Roseires Dam.

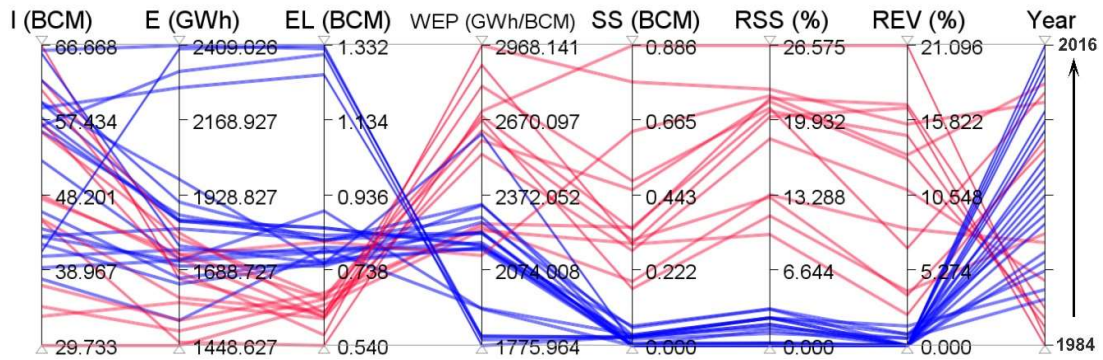


Figure 27 Parallel plots of the historic (1984-2016) water-energy-food-ecosystem nexus indicators. Note: Blue- and red-colored lines represent years with low and high irrigation water shortages, respectively; I = inflow; E = energy generation; EL = evaporation losses; WEP = water-energy productivity; SS = irrigation supply shortages; RSS = risk of irrigation supply shortage; REV = risk to environmental flow violation.

The results show that the steady operation of the GERD would eliminate the irrigation water supply shortages in the study area. This is mainly due to the more regular flow the GERD would provide as shown in Figure 24.

6.4. Water supply to the ecosystem

The annual risk of environmental flow violation (REV) has been used herein to assess the linkages of the ecosystem status with the other nexus components. The REV is the percentage of days in the year where the minimum environmental flow requirements have been violated. Equation 16 was used to calculate the REV.

$$REV = \frac{Dv}{DY} \times 100\% \quad (16)$$

Where:

REV= is the risk of environmental flow violation in the i^{th} year (%)

Dv = the number of days where environmental flow requirements have been violated in the i^{th} year

DY = the number of days in the i^{th} year

In the study area, the minimum environmental outflow from the Sennar Dam is 8 MCM/day, as explained in Section 3.2.3. The blue-colored lines in Figure 28 mark the instances with a low risk of environmental flow violation in the study area. The figure reveals an association between environmental flow provisioning, irrigation water supply, and the hydrologic condition. The highest REV occurred in the year 1985. The heightening of the Roseires Dam reduced the REV significantly.

The analysis of the steady-state operation of the GERD showed that the dam would totally eliminate any risk of environmental flow violation. This is due to the more regular flow that the GERD is expected to provide.

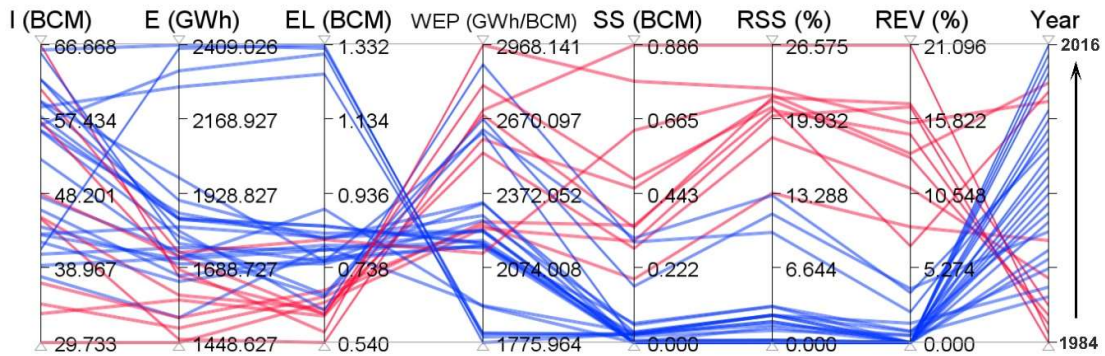


Figure 28 Parallel plots of the historic (1984-2016) water-energy-food-ecosystem nexus indicators. Note: Blue- and red-colored lines represent years with low and high environmental flow violation, respectively; I = inflow; E = energy generation; EL = evaporation losses; WEP = water-energy productivity; SS = irrigation supply shortages; RSS = risk of irrigation supply shortage; REV = risk to environmental flow violation.

7. Conclusions and way forward

The integrative approach of the water-energy-food-ecosystem nexus offers an opportunity to utilize the resources more efficiently by taking into account their interconnections in management and planning. However, there remains an operationalization gap due to the lack of tools and assessment metrics (Liu et al., 2017). This study is an attempt to quantify the interlinkages of the water, energy, food, and ecosystem in resources stressed and data-scarce region. The study region is the Blue Nile Basin downstream the Grand Ethiopian Renaissance Dam. This region has experienced past persistent hydrological droughts, recent dam development, and will soon experience a major dam development in the upstream.

A daily rainfall-runoff and water allocation model has been developed for the study region to quantify some WEF nexus indicators. The model covers the 1984 to 2016 period and includes the major water-related infrastructures and their operating rules. Due to data scarcity in the study region, four satellite-based rainfall products have been evaluated using pixel-to-point approach, and the best performing one was used as a boundary condition to model the rainfall-runoff component of the model. The results show that the African Rainfall Climatology Version 2 (ARC2) has the best performance compared to the other evaluated satellite rainfall products. The historic (1984 to 2016) nexus indicators show an association between environmental flow provisioning, irrigation water supply, and the hydrologic condition. The heightening of the Roseires Dam in 2013 reduced the irrigation supply shortages, reduced the risk of environmental flow violation, increase hydropower generation, increased evaporation losses, and increased the water-energy productivity. The results show that the Grand Ethiopian Renaissance Dam would eliminate the risk of environmental flow violation, eliminate the irrigation supply shortages, increase hydropower generation, increase evaporation losses, and reduce the inter-annual variability in river flow.

The results of this study show a promising role that satellite data can play in filling the data gap in data-scarce regions. A more extensive evaluation of all the available satellite-based rainfall products would be needed to exploit the potential of this emerging data source fully. The analysis conducted herein uses the index-sequential method to analyze future scenarios. However, this method does not take into account nonstationarity in the climate system. Future studies could focus on examining the WEF nexus under transient climate conditions.

8. References

- Abd Elrahim, R.E., 2012. Study of Seasonal Wadi's Flows Entering Roseires and Sennar Reservoirs. University of Khartoum.
- Al-Saidi, M., Elagib, N., 2017. Towards understanding the integrative approach of the water, energy and food nexus. *Science of the Total Environment* 574, 1131–1139. <https://doi.org/10.1016/j.scitotenv.2016.09.046>
- Asadi, A., Boustani, F., 2013. Performance Evaluation of the HEC-HMS Hydrologic Model for Lumped and Semi-distributed Stormflow Simulation (Study Area : Delibajak Basin). *American Journal of Engineering Research (AJER)* 02, 115–121.
- Ashouri, H., Hsu, K., Sorooshian, S., Braithwaite, D., Knapp, K., Cecil, D., Nelson, B., Prat, O., 2015. PERSIANN-CDR: Daily precipitation climate data record from multisatellite observations for hydrological and climate studies. *Bulletin of the American Meteorological Society* 96, 69–83. <https://doi.org/10.1175/BAMS-D-13-00068.1>
- Basheer, M., Elagib, N.A., 2018a. Sensitivity of water-energy nexus to dam operation: A water-energy productivity concept. *Science of the Total Environment* 616–617, 918–926. <https://doi.org/10.1016/j.scitotenv.2017.10.228>
- Basheer, M., Elagib, N.A., 2018b. Performance of satellite-based and GPCC 7.0 rainfall products in an extremely data-scarce country in the Nile Basin. *Atmospheric Research* 215, 128–140. <https://doi.org/10.1016/j.atmosres.2018.08.028>
- Basheer, M., Sulieman, R., Ribbe, L., 2019. Exploring management approaches for water and energy in the data-scarce Tekeze-Atbara Basin under hydrologic uncertainty. *International Journal of Water Resources Development* 1–26. <https://doi.org/10.1080/07900627.2019.1591941>
- Basheer, M., Wheeler, K.G., Ribbe, L., Majdalawi, M., Abdo, G., Zagona, E.A., 2018. Quantifying and evaluating the impacts of cooperation in transboundary river basins on the water-energy-food nexus: The Blue Nile Basin. *Science of the Total Environment* 630, 1309–1323. <https://doi.org/10.1016/j.scitotenv.2018.02.249>
- Bazilian, M., Rogner, H., Howells, M., Hermann, S., Arent, D., Gielen, D., Komor, P., Steduto, P., Mueller, A., Tol, R., Yumkella, K., 2011. Considering the energy, water and food nexus: Towards an integrated modelling approach. *Energy Policy* 39, 7896–7906. <https://doi.org/10.1016/j.enpol.2011.09.039>
- Bhattacharyya, S., Bugatti, N., Bauer, H., 2015. A bottom-up approach to the nexus of energy, food and water security in the Economic Community of West African States (ECOWAS) region.
- Chai, T., Draxler, R., 2014. Root mean square error (RMSE) or mean absolute error (MAE)? -Arguments against avoiding RMSE in the literature. *Geoscientific Model Development* 7, 1247–1250. <https://doi.org/10.5194/gmd-7-1247-2014>
- Diem, J., Hartter, J., Ryan, S., Palace, M., 2014. Validation of Satellite Rainfall Products for Western Uganda. *Journal of Hydrometeorology* 15, 2030–2038. <https://doi.org/10.1175/JHM-D-13-0193.1>

- DIU, 2016. Roseires heightening project [WWW Document]. Ministry of Water Resources and Electricity of Sudan. URL http://www.roseiresdam.gov.sd/en/raising_project.htm (accessed 1.27.19).
- DoP, 2015. Agreement on declaration of principles between the Arab Republic of Egypt, the Federal Democratic Republic of Ethiopia, and the Republic of the Sudan on the Grand Ethiopian Renaissance Dam Project. Khartoum.
- Ebert, E., Janowiak, J., Kidd, C., 2007. Comparison of near-real-time precipitation estimates from satellite observations and numerical models. *Bulletin of the American Meteorological Society* 88, 47–64. <https://doi.org/10.1175/BAMS-88-1-47>
- Elagib, N.A., Gayoum Saad, S.A., Basheer, M., Rahma, A.E., Gore, E.D.L., 2019. Exploring the urban water-energy-food nexus under environmental hazards within the Nile. *Stochastic Environmental Research and Risk Assessment*. <https://doi.org/10.1007/s00477-019-01706-x>
- Endo, A., Tsurita, I., Burnett, K., Orenco, P.M., 2017. A review of the current state of research on the water, energy, and food nexus. *Journal of Hydrology: Regional Studies* 11, 20–30. <https://doi.org/10.1016/j.ejrh.2015.11.010>
- ENTRO, 2006. Multipurpose Development of the Eastern Nile, One–System inventory report on water resource related Data and information Sudan. Khartoum.
- Flammini, A., Puri, M., Pluschke, L., Dubois, O., 2014. Walking the nexus talk: Assessing the water-energy-food nexus in the context of the sustainable energy for all initiative (No. 58), Environment and Natural Resources Working Paper. Rome.
- Funk, C., Peterson, P., Landsfeld, M., Pedreros, D., Verdin, J., Rowland, J., Romero, B., Husak, G., Michaelsen, J., Verdin, A., 2014. A Quasi-Global Precipitation Time Series for Drought Monitoring. U.S. Geological Survey Data Series 832, 4. <https://doi.org/http://dx.doi.org/110.3133/ds832>
- HEC, 2009. HEC-GeoHMS Geospatial Hydrologic Modeling Extension: User’s Manual. Washington.
- HEC, 2008. Hydrologic Modeling System HEC-HMS Applications Guide. Washington, D.C.
- Hoff, H., 2011. Understanding the Nexus. Background Paper for the Bonn2011 Conference: The Water, Energy and Food Security Nexus. Stockholm Environment Institute. Stockholm.
- Howells, M., Hermann, S., Welsch, M., Bazilian, M., Segerström, R., Alfstad, T., Gielen, D., Rogner, H., Fischer, G., van Velthuizen, H., Wiberg, D., Young, C., Roehrl, R., Mueller, A., Steduto, P., Ramma, I., 2013. Integrated analysis of climate change, land-use, energy and water strategies. *Nature Climate Change* 3, 621–626. <https://doi.org/10.1038/nclimate1789>
- IWMI, 2012. The Nile River Basin water, Agriculture, Governance and Livelihoods, 1st ed. Routledge, Oxon.
- Jarvis, A., Reuter, H., Nelson, A., Guevara, E., 2008. Hole-filled SRTM for the globe Version 4 [WWW Document]. CGIAR-CSI SRTM 90m Database. URL <http://srtm.csi.cgiar.org>

(accessed 12.30.18).

- Kendall, D., Dracup, J., 1991. A comparison of index-sequential and AR(1) generated hydrologic sequences. *Journal of Hydrology* 122, 335–352. [https://doi.org/10.1016/0022-1694\(91\)90187-M](https://doi.org/10.1016/0022-1694(91)90187-M)
- Keskinen, M., Someth, P., Salmivaara, A., Kummu, M., 2015. Water-energy-food nexus in a transboundary river basin: The case of Tonle Sap Lake, Mekong River Basin. *Water* 7, 5416–5436. <https://doi.org/10.3390/w7105416>
- Kibaroglu, A., Gürsoy, S., 2015. Water–energy–food nexus in a transboundary context: the Euphrates–Tigris river basin as a case study. *Water International* 40, 824–838. <https://doi.org/10.1080/02508060.2015.1078577>
- Legates, D., McCabe Jr, G., 1999. Evaluating the Use of “Goodness of Fit” Measures in Hydrologic and Hydroclimatic Model Validation. *Water Resources Research* 35, 233–241. <https://doi.org/10.1029/1998WR900018>
- Lindström, A., Granit, J., 2012. Large-scale water storage in the water, energy and food nexus Perspectives on benefits, risks and best practices.
- Liu, J., Yang, H., Cudennec, C., Gain, A.K., Hoff, H., Lawford, R., Qi, J., de Strasser, L., Yillia, P.T., Zheng, C., 2017. Challenges in operationalizing the water–energy–food nexus. *Hydrological Sciences Journal* 62, 1714–1720. <https://doi.org/10.1080/02626667.2017.1353695>
- Maidment, R., Grimes, D., Allan, R., Tarnavsky, E., Stringer, M., Hewison, T., Roebeling, R., Black, E., 2014. The 30 year TAMSAT African Rainfall Climatology And Time series (TARCAT) data set. *Journal of Geophysical Research: Atmospheres* 119, 10619–10644. <https://doi.org/10.1002/2014JD021927>
- MIT, 2014. The Grand Ethiopian Renaissance Dam: An opportunity for collaboration and shared benefits in the Eastern Nile Basin, An mmicus brief to the riparian Nations of Ethiopia, Sudan and Egypt From the international, non-partisan Eastern Nile Working Group. Cambridge.
- Modarres, R., 2007. Streamflow drought time series forecasting. *Stochastic Environmental Research and Risk Assessment* 21, 223–233. <https://doi.org/10.1007/s00477-006-0058-1>
- Mohamed, Y., Loulseged, M., 2008. The Nile Basin Water Resources : Overview of Key Research Questions Pertinent to the Nile Basin Initiative. Colombo.
- Mohammed, K., 2015. Ma’akhz wathiqat i’lan almbade’ hawla sad alnahda men almontalaq alilmy alhandasy [Reservations on the Declaration of Principles on GERD from a technical point of view] [WWW Document]. Sudacon. URL http://www.sudacon.net/2015/04/blog-post_6.html (accessed 11.17.18).
- MolHES, 1977. Blue Nile Waters Study Phase IA: Availability and use of Blue Nile Water. Khartoum.
- MolHPS, 1966. Roseires Dam. Khartoum.
- Mu, Q., Zhao, M., Running, S., 2011. Improvements to a MODIS global terrestrial

- evapotranspiration algorithm. *Remote Sensing of Environment* 115, 1781–1800. <https://doi.org/10.1016/j.rse.2011.02.019>
- NBI, 2012. State of the River Nile Basin. Nile Basin Initiative, Entebbe.
- Novella, N., Thiaw, W., 2013. African rainfall climatology version 2 for famine early warning systems. *Journal of Applied Meteorology and Climatology* 52, 588–606. <https://doi.org/10.1175/JAMC-D-11-0238.1>
- Ouarda, T., Labadie, J., Fontane, D., 1997. Indexed sequential hydrologic modeling for hydropower capacity estimation. *Journal of the American Water Resources Association* 33, 1337–1349.
- Pittock, J., Dumaresq, D., Bassi, A., 2016. Modeling the hydropower–food nexus in large river basins: A Mekong case study. *Water* 8. <https://doi.org/10.3390/w8100425>
- R Core Team, 2015. R: A Language and Environment for Statistical Computing [WWW Document]. URL at: <https://www.R-project.org/> (accessed 6.27.17).
- Ribbe, L., Ahmed, S., 2006. Transboundary Water Resources Issues in the Nile River Basin, in: *Management Technology, Resource Management and Development*, Wasser Berlin. Berlin, pp. 13–26.
- Roseires Dam Heightening Unit, 2005. Updating economic and financial viability study of dam heightening. Khartoum.
- Salini Impregilo, 2016. Grand Ethiopian Renaissance Dam Project [WWW Document]. URL <http://www.salini-impregilo.com/en/projects/in-progress/dams-hydroelectric-plants-hydraulic-works/grand-ethiopian-renaissance-dam-project.html> (accessed 6.22.19).
- Salman, S., 2016. The Grand Ethiopian Renaissance Dam: the road to the declaration of principles and the Khartoum document. *Water International* 41, 512–527. <https://doi.org/10.1080/02508060.2016.1170374>
- Stamou, A., Rutschmann, P., 2018. Pareto Optimization of Water Resources Using the Nexus Approach. *Water Resources Management*. <https://doi.org/10.1007/s11269-018-2127-x>
- Stern, M., Flint, L., Minear, J., Flint, A., Wright, S., 2016. Characterizing changes in streamflow and sediment supply in the Sacramento River Basin, California, using hydrological simulation program—FORTRAN (HSPF). *Water* 432, 1–21. <https://doi.org/10.3390/w8100432>
- Strasser, L., Lipponen, A., Howells, M., Stec, S., Bréthaut, C., 2016. A Methodology to Assess the Water Energy Food Ecosystems Nexus in Transboundary River Basins. *Water* 8. <https://doi.org/10.3390/w8020059>
- Sulieman, H., Mohammed, M., 2014. Patterns of Woody Plant Species Composition and Diversity in Dinder National Park, Sudan, *University of Kordofan Journal of Natural Resources and Environmental Studies*, UKJNRES.
- Sutcliffe, J., Parks, Y., 1999. The hydrology of the Nile, *International Association of Hydrological Sciences*. The International Association of Hydrological Science,

Wallingford.

- Swanson, A., 2014. The Grand Ethiopian Renaissance Dam: Sustainable development or not?, Virginia Tech, Center for Leadership in Global Sustainability (CLiGS). Arlington.
- Tawfik, R., 2016. The Grand Ethiopian Renaissance Dam: a benefit-sharing project in the Eastern Nile? *Water International* 8060, 1–19. <https://doi.org/10.1080/02508060.2016.1170397>
- Toté, C., Patricio, D., Boogaard, H., van der Wijngaart, R., Tarnavsky, E., Funk, C., 2015. Evaluation of satellite rainfall estimates for drought and flood monitoring in Mozambique. *Remote Sensing* 7, 1758–1776. <https://doi.org/10.3390/rs70201758>
- UN, 2018. Sustainable development goal 6: Synthesis report on water and sanitation 2018. New York. <https://doi.org/10.1126/science.278.5339.827>
- UN, 2015a. World Population Prospects: Key Findings and Advance Tables (No. ESA/P/WP.241). New York.
- UN, 2015b. The Millennium Development Goals Report, United Nations. New York.
- UNDP, 2015. Human Development Report 2015: Work for Human Development. New York.
- UNEP, 2010. Stock Taking of Adaptation Activities in the Nile River Basin. Nairobi.
- WEHAB Working Group, 2002. A Framework for Action on Energy, World summit on sustainable development. Johannesburg.
- Wheeler, K., Hall, J., Abdo, G., Dadson, S., Kasprzyk, J., Smith, R., Zagona, E., 2018. Exploring cooperative transboundary river management strategies for the Eastern Nile Basin. *Water Resources Research* 9224–9254. <https://doi.org/10.1029/2017WR022149>
- Wheeler, K.G., Basheer, M., Mekonnen, Z., Eltoun, S., Mersha, A., Abdo, G., Zagona, E., Hall, J., Dadson, S., 2016. Cooperative filling approaches for the Grand Ethiopian Renaissance Dam. *Water International* 8060, 1–24. <https://doi.org/10.1080/02508060.2016.1177698>
- WMO, 2016. Country Profile Database [WWW Document]. URL <https://www.wmo.int/cpdb/sudan> (accessed 5.23.17).
- Woldesenbet, T.A., Elagib, N.A., Ribbe, L., Heinrich, J., 2017. Hydrological responses to land use/cover changes in the source region of the Upper Blue Nile Basin, Ethiopia. *Science of the Total Environment* 575, 724–741. <https://doi.org/10.1016/j.scitotenv.2016.09.124>
- World Economic Forum, 2011. Global Risks: An initiative of the Risk Response Network. Geneva.
- Zagona, E., Fulp, T., Shane, R., Magee, T., Goranflo, H.M., 2001. Riverware: a generalized tool for complex reservoir system modeling. *Journal of the American Water Resources Association* 37, 913–929.
- Zagona, E., Rajagopalan, B., Setzer, S., 2008. Riverware Decision Support Tools for Planning Sustainable River Development with Hydropower, in: High-Level International Forum on Water Resources and Hydropower. Beijing, pp. 1–8.

- Zambrano-Bigiarini, M., Nauditt, A., Birkel, C., Verbist, K., Ribbe, L., 2017. Temporal and spatial evaluation of satellite-based rainfall estimates across the complex topographical and climatic gradients of Chile. *Hydrology and Earth System Sciences* 21, 1295–1320. <https://doi.org/10.5194/hess-21-1295-2017>
- Zhang, Z., Xu, C.-Y., Yong, B., Hu, J., Sun, Z., 2012. Understanding the changing characteristics of droughts in Sudan and the corresponding components of the hydrologic cycle. *Journal of Hydrometeorology* 13, 1520–1535. <https://doi.org/10.1175/JHM-D-11-0109.1>